Phytophthora infestans RXLR Effector AVR1 Interacts with Exocyst Component Sec5 to Manipulate Plant Immunity[1][OPEN]

Yu Du, Mohamed H. Mpina[2], Paul R.J. Birch, Klaas Bouwmeester[3], and Francine Govers[3]*

Laboratory of Phytopathology, Wageningen University, 6708 PB, Wageningen, The Netherlands (Y.D., M.H.M., K.B., F.G.); Division of Plant Sciences, College of Life Science, University of Dundee at the James Hutton Institute, Invergowrie, Dundee, United Kingdom (P.R.J.B.); and Plant-Microbe Interactions, Department of Biology, Faculty of Science, Utrecht University, 3584 CH, Utrecht, The Netherlands (K.B.)

ORCID IDs: 0000-0002-3512-0200 (Y.D.); 0000-0002-6559-3746 (P.R.J.B.); 0000-0002-8141-3880 (K.B.); 0000-0001-5311-929X (F.G.).

Phytophthora infestans secretes numerous RXLR effectors that modulate host defense and thereby pave the way for successful invasion. Here, we show that the RXLR effector AVR1 is a virulence factor that promotes colonization and suppresses callose deposition, a hallmark of basal defense. To identify host targets of AVR1, we performed yeast two-hybrid screens and selected Sec5 as a candidate. Sec5 is a subunit of the exocyst, a protein complex that is involved in vesicle trafficking. AVR1-like (A-L), a close homolog of AVR1, also acts as a virulence factor, but unlike AVR1, A-L does not suppress CRINKLER2 (CRN2)-induced cell death or interact with Sec5. Compared with AVR1, A-L is shorter and lacks the carboxyl-terminal tail, the T-region that is crucial for CRN2-induced cell death suppression and Sec5 interaction. In planta analyses revealed that AVR1 and Sec5 are in close proximity, and coimmunoprecipitation confirmed the interaction. Sec5 is required for secretion of the pathogenesis-related protein PR-1 and callose deposition and also plays a role in CRN2-induced cell death. Our findings show that *P. infestans* manipulates an exocyst subunit and thereby potentially disturbs vesicle trafficking, a cellular process that is important for basal defense. This is a novel strategy that oomycete pathogens exploit to modulate host defense.

Phytophthora spp. are oomycete plant pathogens that are widespread and able to infect a vast group of plants, including many economically important crops (Kroon et al., 2012). The most infamous species is *Phytophthora infestans*, the late blight pathogen that causes great losses in potato (*Solanum tuberosum*) and tomato (*Solanum lycopersicum*) production worldwide. To establish infection and subsequent colonization of host tissue, *P. infestans* secretes effectors that manipulate the host cell machinery to suppress defense responses. A better insight into how pathogen effectors modulate host defense would help in designing more targeted strategies toward improving disease resistance in crops.

P. infestans has a remarkably large number of genes encoding secreted effector proteins, including RXLR effectors and CRINKLERS (CRNs) that exhibit short conserved N-terminal motifs required for host cell translocation (Haas et al., 2009; Stassen and Van den Ackerveken, 2011). The 240-Mb genome of *P. infestans* contains approximately 560 RXLR effector genes and over 180 CRN genes (Haas et al., 2009), and this is significantly more than in any other oomycete sequenced to date. Emerging evidence indicates that RXLR effectors have dual activities. On the one hand, RXLR effectors are able to suppress plant defense responses (Bos et al., 2006; Oh et al., 2009; Halterman et al., 2010), in particular pathogen-associated molecular pattern-triggered immunity (PTI) elicited by pathogen-associated molecular patterns (Jones and Dangl, 2006) or elicitor-triggered cell death (Bos et al., 2006). On the other hand, RXLR effectors are able to activate plant defense responses. This so-called effector-triggered immunity is often a very strong response reminiscent of a hypersensitive response (HR) leading to local cell death (Jones and Dangl, 2006; Hardham and Cahill, 2010). This response only occurs when the plant has a resistance (R) protein that specifically recognizes one of the RXLR effectors. The conserved RXLR motif was first discovered in a set of diverse secreted oomycete proteins that shared the ability to elicit

[1] This work was supported by the China Scholarship Council (fellowship to Y.D.), by the Technology Foundation of the Netherlands Organization for Scientific Research (VENI grant to K.B.), and by the Food-for-Thought-Thought-for-Food Campaign from the Wageningen University Fund.

[2] Present address: Plant Protection Division, Tropical Pesticides Research Institute, 3024 Arusha, Tanzania.

[3] These authors contributed equally to the article.

* Address correspondence to francine.govers@wur.nl.

The author responsible for distribution of materials integral to the findings presented in this article in accordance with the policy described in the Instructions for Authors (www.plantphysiol.org) is: Francine Govers (francine.govers@wur.nl).

Y.D., P.R.J.B., K.B., and F.G. designed the research; Y.D., M.H.M., and K.B. performed the experiments; Y.D., K.B., and F.G. analyzed the data; Y.D, K.B., and F.G. wrote the article; P.R.J.B. complemented the writing.

[OPEN] Articles can be viewed without a subscription.

www.plantphysiol.org/cgi/doi/10.1104/pp.15.01169

an effective defense response in plants carrying specific *R* genes (Rehmany et al., 2005). In *P. infestans*, a number of RXLR effectors, including AVR1, AVR2, AVR3a, AVR4, IPI-O1 (AVR-blb1), AVR-blb2, and AVR-vnt1, have been demonstrated to act as avirulence factors according to this classical gene-for-gene model (Flor, 1971; Vleeshouwers et al., 2011), and in most cases their corresponding *R* genes have been identified. The first one to be cloned was *R1*, which, like other late blight *R* genes, encodes an intracellular NUCLEOTIDE-BINDING DOMAIN/LEUCINE-RICH REPEAT (NLR) protein (Ballvora et al., 2002; Vleeshouwers et al., 2011). Despite the fact that the term avirulence factor has become obsolete, the nomenclature of several RXLR effector genes still refers to the original concept of the gene-for-gene model.

This study deals with *AVR1*, a *P. infestans* gene identified by map-based cloning, and based on its ability to elicit an HR when coexpressed with *R1* in *Nicotiana benthamiana* (Guo, 2008). *AVR1* encodes a 208-amino acid protein consisting of a signal peptide, an RXLR domain, and a C-terminal region that determines its effector activity. Similar to other RXLR effectors, the C-terminal region of AVR1 lacks homology to any other protein but has two W motifs and one Y motif, conserved motifs that have been identified in over 700 RXLR effectors (Jiang et al., 2008). *P. infestans* isolates that are virulent on *R1* potato plants lack the *AVR1* locus but possess a homologous gene named *AVR1-like* (*A-L*) at another locus. At the protein level, A-L shows 82% homology to AVR1. Similar to AVR1, A-L has an RXLR domain, two W motifs, and one Y motif but is shorter; it lacks a 38-amino acid tail at the C terminus, here referred to as the T-region. Unlike AVR1, A-L is not able to trigger R1-mediated resistance, likely due to the numerous polymorphisms in the effector domain and the missing T-region (Du et al., 2015).

Plants have developed multiple defense strategies to inhibit pathogen invasion. It is clear that the plant secretory pathway is involved in defense because of the secretion of antimicrobial compounds to the apoplast (Robatzek, 2007), and there is increasing evidence that vesicle trafficking is important for an effective immune response. For example, the plasma membrane-associated syntaxins NbSYP132 and PENETRATION1 (PEN1; or SYP121), known as soluble NSF attachment protein receptors (SNAREs), were reported to be required for accumulation of the pathogenesis-related protein PR-1 in the apoplast and for assembly of papillae and focal secretion, respectively (Collins et al., 2003; Kalde et al., 2007). One step upstream of SNAREs is the exocyst, which tethers post-Golgi vesicles to the plasma membrane (He and Guo, 2009). The exocyst, which was initially discovered in yeast, is a protein complex consisting of eight subunits (Hsu et al., 1996; TerBush et al., 1996). Its function is extensively studied in yeast and animals (Hsu et al., 2004). In contrast, the plant exocyst is less well studied but is known to be essential for plant development and involved in polarized secretion and exocytosis (Cole et al., 2005; Wen et al., 2005; Synek et al., 2006; Hála et al., 2008). More recent reports point to roles in plant defense, including cell wall apposition formation, PTI, and suppression of spontaneous HR mediated by salicylic acid (SA; Pecenková et al., 2011; Stegmann et al., 2012; Kulich et al., 2013). An anticipated role of vesicle trafficking and the exocyst in defense is further supported by the findings of Zhao et al. (2015), who showed physical interaction between a truncated NLR protein and one of the exocyst subunits, and by the observation that several pathogen effectors target the vesicle-trafficking machinery in the host to facilitate colonization. For example, HopM1 from *Pseudomonas syringae* destabilizes Arabidopsis (*Arabidopsis thaliana*) AtMIN7, an ADP ribosylation factor guanine nucleotide-exchange factor and a key regulator of vesicle formation, and this destabilization leads to enhanced pathogen colonization (Nomura et al., 2006, 2011). The *P. syringae* effector HopZ2 targets Arabidopsis MLO2 to suppress PEN1-dependent secretion of defense components (Lewis et al., 2012). WtsE, an AvrE family type III effector secreted by the maize (*Zea mays*) pathogen *Pantoea stewartii* ssp. *stewartii*, carries a putative endoplasmic reticulum membrane localization signal that is important for its virulence function, such as forming water-soaked lesions and inducing necrosis (Ham et al., 2006). The fungal plant pathogen *Alternaria carthami* secretes the phytotoxin brefeldin A that inhibits the formation of Golgi-derived vesicles (Driouich et al., 1997). Brefeldin A impedes Arabidopsis penetration resistance by blocking callose deposition and the accumulation of syntaxin PEN1 at the plasma membrane (Nielsen et al., 2012).

To date, a number of RXLR effectors have been exploited to study the mechanisms by which oomycetes manipulate host immunity, and the results show that these mechanisms vary. *Phytophthora sojae* Avh331 and various *P. infestans* RXLR effectors were found to modulate mitogen-activated protein kinase signaling to suppress plant immunity (Cheng et al., 2012; King et al., 2014; Zheng et al., 2014). *P. sojae* AVR3b, which has NADH and ADP-ribose pyrophosphorylase activity, manipulates host immunity by interfering with effector-triggered immunity (Dong et al., 2011). The *Phytophthora parasitica* RXLR effector PENETRATION-SPECIFIC EFFECTOR1 promotes colonization by impeding host auxin physiology (Evangelisti et al., 2013). The *P. infestans* RXLR effector IPI-O1 disrupts the integrity of adhesions between the plasma membrane and the cell wall and uses the membrane-spanning lectin receptor kinase LecRK-I.9 as a host target (Bouwmeester et al., 2011). *P. infestans* AVR3a^{KI} stabilizes the host E3 ligase CMPG1, thereby modulating host immunity (Bos et al., 2010). *P. infestans* Pi03192 hampers the relocalization of two host transcription factors to promote pathogen colonization (McLellan et al., 2013). *P. infestans* AVR-blb2 is able to inhibit the secretion of the plant immune protease C14 to the haustorial interface (Bozkurt et al., 2011), indicating that effectors can have the ability to interfere with plant focal secretion. However, as yet, there are no reports of oomycete pathogen effectors that specifically target the vesicle-trafficking machinery to modulate the host immune system.

The aim of this study was to investigate the ability of AVR1 to promote virulence and to unravel the mechanism by which AVR1 manipulates host defense. Yeast two-hybrid (Y2H) assays were carried out to identify host proteins interacting with AVR1. One of the candidates selected as a potential host target of AVR1 was the exocyst component Sec5. Characterization of the Sec5-AVR1 interaction in planta revealed that AVR1 stabilizes Sec5. Sec5 is involved in plant defense against *P. infestans*. Altogether, these findings point to a novel strategy that oomycete pathogens exploit to modulate host defense and that is manipulating proteins that are part of the vesicle-trafficking machinery.

RESULTS

The RXLR Effectors AVR1 and A-L Promote in Planta Growth of *P. infestans*

To test whether AVR1 and A-L contribute to *P. infestans* colonization, we transiently expressed the effector genes in *N. benthamiana* leaves via agroinfiltration and subsequently performed infection assays. Detached leaves of *N. benthamiana* plants transiently expressing AVR1-myc, A-L-myc, or GUS were inoculated with zoospores from *P. infestans* isolate 88069. In the early biotrophic stage of the interaction, *P. infestans* forms lesions that gradually start to sporulate. Only in later stages, the host cells in the center of lesions start to die and the lesions become necrotic. Lesion diameters were measured at 6 d after inoculation (dai), and lesion areas were calculated. The presence of AVR1 or A-L resulted in larger lesions (Fig. 1A), suggesting that both RXLR effectors enhance *Phytophthora* proliferation in planta and, as such, serve as genuine virulence factors.

The T-Region of AVR1 Promotes *P. infestans* Colonization

The C-terminal domain of AVR1 comprises three motifs (W1, W2, and Y), two linker regions (ln1 and ln2), and at the very end the T-region that is absent in A-L (Fig. 1C). To investigate which motifs of AVR1 and A-L are required to promote *P. infestans* colonization, various deletion and chimeric constructs were made and transiently expressed in *N. benthamiana* leaves. Subsequent infection assays confirmed that AVR1 and A-L promote the in planta growth of *P. infestans* and showed that truncation of the T-region ($AVR1^{\Delta T}$) abolishes the ability of AVR1 to promote growth (Fig. 1, B and D). Remarkably, the T-region by itself is sufficient to promote *P. infestans* colonization and can even slightly boost the growth promotion when fused as a C-terminal tail to A-L ($A\text{-}L^{ST}$).

Suppression of CRN2-Induced Cell Death by AVR1 Depends on the T-Region

Since the virulence activity of AVR1 might be correlated with its ability to suppress the activity of other effectors, we tested whether AVR1 is able to suppress cell death induced by CRN2. CRN2, a protein secreted by *P. infestans*, is a potent cell death inducer (Torto et al., 2003), and when infiltrated in *N. benthamiana*, we indeed observed a strong response. At 4 d post infiltration (dpi), more than 80% of the sites infiltrated with CRN2 showed cell death (Fig. 1E), whereas sites infiltrated with GUS did not show this response. However, when coinfiltrated with AVR1-myc, the response was significantly reduced: only 50% of the infiltrated sites developed CRN2-induced cell death. To determine which motif or region in AVR1 is responsible for this suppression, we tested A-L and the various chimeric and deletion constructs. Upon coinfiltration of CRN2 with either A-L or $AVR1^{\Delta T}$, there was no cell death suppression; all or nearly all sites developed cell death, suggesting that the T-region is important for cell death suppression. Indeed, when coinfiltrating with the T-region by itself or the T-region fused as the C-terminal tail to A-L ($A\text{-}L^{ST}$), CRN2-induced cell death was suppressed in over 50% of the infiltrated sites (Fig. 1E). Testing a more extensive set of deletion and chimeric constructs revealed that the T-region of AVR1 is the pivotal determinant for the suppression of CRN2-induced cell death. All chimeric constructs containing the T-region were able to suppress cell death but none of the constructs lacking the T-region were, and this was independent of the origin of the conserved motifs, as was further confirmed by the W1 deletion construct that also retained its activity as a suppressor (Supplemental Fig. S1).

AVR1 Interacts with Plant Exocyst Component Sec5

To identify host targets of AVR1, Y2H screenings were performed. This resulted in a set of clones coding for potato proteins potentially interacting with AVR1, including three encoding the exocyst component Sec5. One (named StSec5-a) harbors a complementary DNA (cDNA) insert encoding an almost full-length Sec5 protein with only three amino acids missing at the N terminus (Supplemental Fig. S2). Based on alignments with known *Sec5* sequences, primers were designed for obtaining a full-length potato *Sec5* cDNA clone (StSec5). To investigate the interaction specificity between Sec5 and AVR1, we cotransformed the prey plasmid containing *StSec5* with bait plasmids containing *AVR1*, *A-L*, *IPI-O1*, or *IPI-O4*. This confirmed the Sec5-Avr1 interaction in yeast and showed that this interaction is specific; only AVR1 interacts with Sec5 and none of the other three RXLR effectors (Fig. 2A). Cotransformation of the nearly full-length and the partial *StSec5* clones with the four RXLR effectors confirmed that Sec5 specifically interacts with AVR1 (Supplemental Fig. S3).

To investigate whether AVR1 and Sec5 interact in planta, full-length StSec5 with an N-terminal GFP tag (GFP-StSec5) and AVR1 with a C-terminal myc tag (AVR1-myc) were coexpressed in *N. benthamiana* leaves. Coimmunoprecipitation was performed at 3 dpi. The

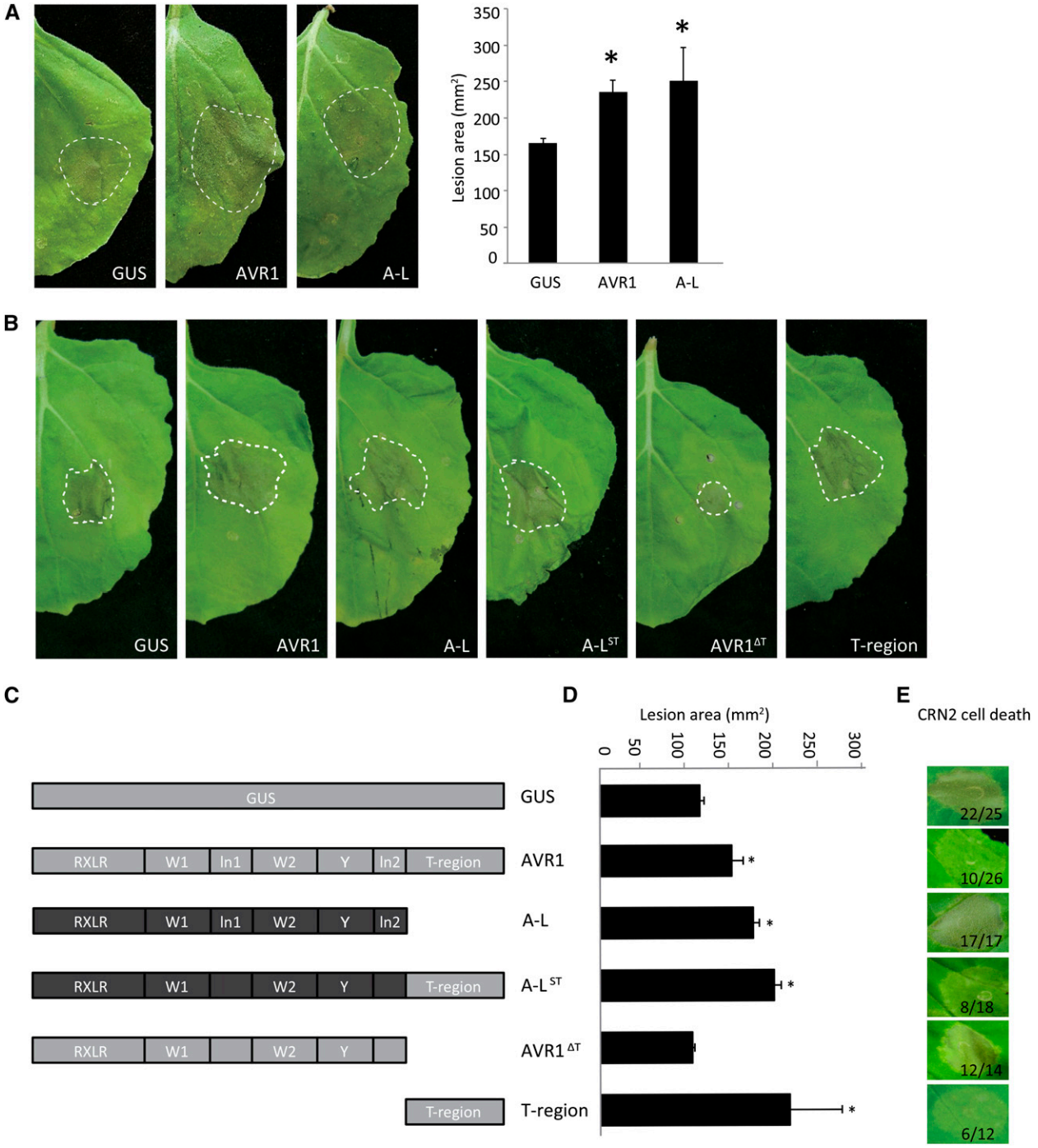

Figure 1. Transient expression of AVR1 in *N. benthamiana* promotes the in planta growth of *P. infestans* and suppresses CRN2-induced cell death. A, *Agrobacterium tumefaciens* strains carrying GUS, AVR1-myc (AVR1), and A-L-myc (A-L) constructs were infiltrated in leaves, and after 24 h, the leaves were inoculated with zoospores of *P. infestans* isolate 88069. Photographs were taken at 6 dai. Asterisks indicate significant differences from the GUS control ($n \geq 9$; one-sided Student's *t* test, $P < 0.05$). B, *A. tumefaciens* strains carrying the constructs shown in C were infiltrated in leaves, and after 24 h, the leaves were inoculated with zoospores of *P. infestans* isolate 14-3-GFP. Photographs were taken at 6 dai, and lesion sizes were measured (see D). C, Schematic drawings of AVR1 and A-L, the chimeric version A-LST, and two truncated versions, AVR1$^{\Delta T}$ and T-region. D, Measurements of the lesions shown in B. The bars reflect the lesion areas in mm^2. Error bars are from nine replicates. The experiments were repeated three times with similar results. Asterisks indicate significant differences from the GUS control ($n \geq 9$; one-sided Student's *t* test, $P < 0.05$). E, *A. tumefaciens* stains carrying the constructs shown in C were coagroinfiltrated with CRN2, and cell death was monitored at 4 dpi. The numbers show the ratio of infiltrated sites that developed cell death versus the total number of infiltrated sites.

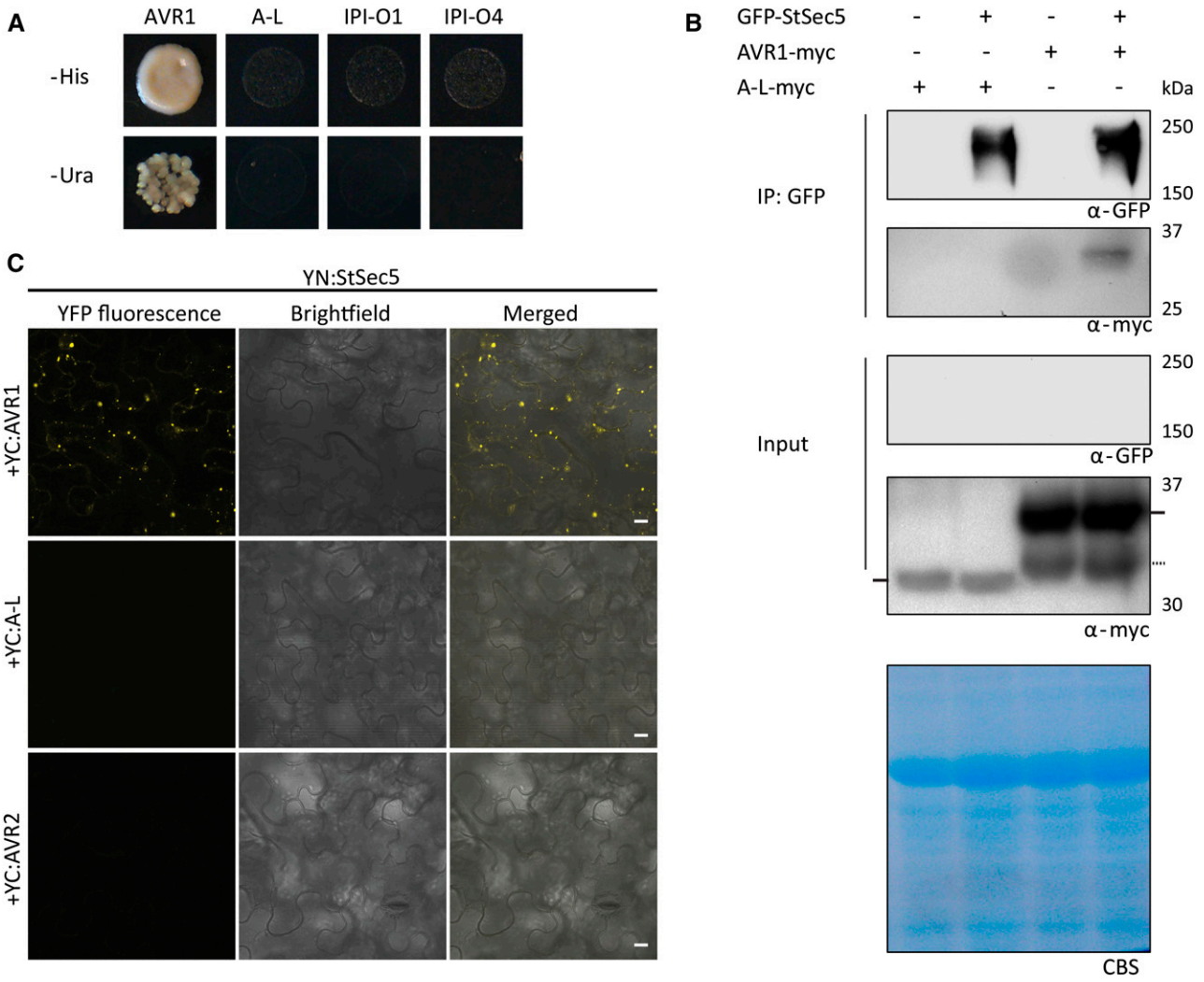

Figure 2. The *P. infestans* RXLR effector AVR1 specifically associates with Sec5. A, *P. infestans* AVR1 interacts with potato Sec5 (StSec5) in yeast. Cotransformation of yeast is shown with a Y2H prey vector containing Sec5 and a Y2H bait vector containing AVR1, A-L, IPI-O1, or IPI-O4 as indicated. Only the coexpression of Sec5 and Avr1 resulted in growth on medium lacking His (−His) or uracil (−Ura). B, Coimmunoprecipitation showing that AVR1 interacts with StSec5 in planta. Total protein extracts (Input) of *N. benthamiana* leaves infiltrated with the indicated constructs (+), and protein complexes immunoprecipitated with GFP-trap_A beads (IP: GFP) were separated on gels and blotted. GFP- and myc-tagged fusion proteins were detected by probing western blots with GFP and myc antibodies. In the total protein extracts, the bands representing A-L and AVR1 are indicated by horizontal bars at the left and right, respectively. The dotted horizontal bar at the right points to a breakdown product of AVR1. Only AVR1 is detected in a complex with StSec5. CBS, Coomassie Blue staining of the blot containing total protein extracts showed equal loading in each lane based on the 50-kD Rubisco band. C, BiFC confirms that AVR1 interacts with StSec5. The C terminus of YFP (YC) was fused to the N terminus of AVR1, A-L, and AVR2, and the N terminus (YN) of YFP was fused to the N terminus of StSec5. YN:StSec5 was coexpressed with YC:AVR1, YC:A-L, and YC:AVR2 in *N. benthamiana* leaves. Images were taken using confocal microscopy at 2 dpi. Bars = 10 μm.

results show that AVR1-myc coimmunoprecipitates with GFP-StSec5 while A-L-myc does not (Fig. 2B). A-L-myc is present in the input; however, compared with AVR1-myc, there is less and it cannot be excluded that the level in the coimmunoprecipitated fraction is too low to be detected. In the absence of GFP-StSec5, AVR1-myc is not coimmunoprecipitated by anti-GFP-conjugated agarose, demonstrating that AVR1 is specifically associated with a complex that contains StSec5 (Fig. 2B). Taken together, these results show that AVR1 associates with Sec5 in planta. To ensure the presence of StSec5, we immunoprecipitated StSec5 with GFP beads, performed on-bead trypsin digestion, and analyzed the resulting peptides by mass spectrometry. Based on the more or less even distribution of peptides on the Sec5 protein, we conclude that the full-length Sec5 protein is produced (Supplemental Fig. S4).

To find additional support for the in planta interaction between Sec5 and AVR1, we performed bimolecular fluorescence complementation (BiFC). N- or

C-terminal portions of yellow fluorescent protein (YFP) coding sequences were fused to *AVR1*, *A-L*, *AVR2*, or *StSec5*, and constructs that harbor complementary portions of YFP were coexpressed in *N. benthamiana* leaves. Confocal microscopy revealed that a combination of YC:AVR1 and YN:StSec5 restored YFP fluorescence (Fig. 2C). This confirms that, in planta, AVR1 and StSec5 are in close proximity. In contrast, no YFP fluorescence was observed when YC:A-L or YC:AVR2 was coexpressed with YN:StSec5, again pointing to specificity between Sec5 and AVR1. The expression levels of effector proteins were shown by western blot probed with appropriate antibodies and are shown in Supplemental Figure S5.

The T-Region of AVR1 Is Required for Sec5 Binding in Yeast

In yeast, Sec5 interacts with AVR1 but not with A-L. To determine which motif or region in AVR1 is needed for the interaction with Sec5, Y2H assays were performed using various AVR1 and A-L chimeric and deletion constructs as bait vector. Cotransformation of these bait constructs with Sec5 as prey showed that a yeast transformant containing the deletion construct AVR1$^{\Delta T}$ was unable to grow on selection medium, indicating that in the absence of the T-region, AVR1 loses its ability to bind Sec5. However, the T-region by itself also failed to interact with Sec5, as did the chimeric protein in which the T-region of AVR1 is fused to A-L (A-LST; Fig. 3). Because this suggested that motifs other than the T-region are required for physical interaction, we analyzed a more extensive set of chimeric bait constructs (Fig. 3). This revealed that Sec5 interaction is only lost when the Y motif of AVR1 is replaced by the Y motif of A-L. In conclusion, both the Y motif and the T-region of AVR1 are essential for interaction with Sec5.

Sec5 Silencing Reduces Plant Growth and Alters Leaf Development

To get insight into the function of Sec5, we set out to obtain *N. benthamiana* and tomato plants with reduced Sec5 levels by exploiting tobacco rattle virus (TRV) for virus-induced gene silencing (VIGS). For identifying target sequences for VIGS, we first investigated the Sec5 distribution in solanaceous plants and aligned the sequences. Unlike yeast and animals with single-copy genes for each exocyst subunit, plants have multiple genes for over half of the exocyst subunits, including Sec5 (Synek et al., 2006; Zhang et al., 2010). Phylogenetic analysis revealed two distinct clades, one containing plant Sec5 proteins and the other grouping the animal Sec5s (Supplemental Fig. S6). Similar to Arabidopsis, tomato and potato each have two *Sec5* genes, whereas *N. benthamiana* with its allopolyploid genome has four. Because of the high conservation, we were able to generate a VIGS construct that targets all the *N. benthamiana* and tomato *Sec5* homologs (Supplemental Fig. S7). Quantitative reverse transcription (Q-RT)-PCR analyses showed strongly reduced levels of *Sec5* mRNA, reaching on average only 16% of the normal

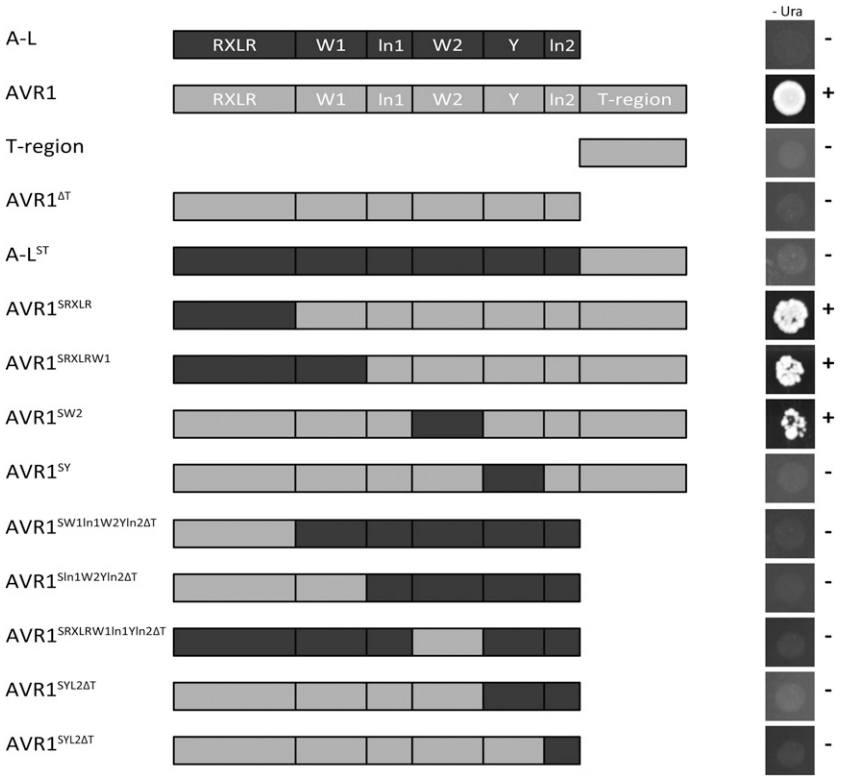

Figure 3. The T-region of AVR1 is indispensable for interaction with Sec5 in yeast. Cotransformation of yeast is shown with a Y2H prey vector containing potato Sec5 (StSec5) and Y2H bait vectors containing AVR1, A-L, the T-region, AVR1 lacking the T-region (AVR1$^{\Delta T}$), or various chimeric derivatives as depicted. A strong interaction between prey and bait enables growth (+) on medium lacking uracil (–Ura).

level in *N. benthamiana* (Fig. 4B) and 36% of the normal level in tomato (Supplemental Fig. S8B). The transcript levels of each of the four individual *N. benthamiana Sec5* genes appeared to be reduced, while *Sec3* and *Exo70E2* transcript levels were not affected (Supplemental Fig. S9). This demonstrates that, indeed, the VIGS construct is *Sec5* specific and targets all *Sec5* homologs.

In both plant species, silencing of *Sec5* altered plant growth (Fig. 4A; Supplemental Fig. S8A). *Sec5*-silenced plants (TRV:*Sec5*) were smaller when compared with control plants (TRV:*GUS*), and in particular in *N. benthamiana*, the first six leaves were smaller and thicker while the upper younger leaves were small and curved. As a control, we also silenced *SGT1*, a gene encoding a chaperone protein that is required for HR-mediated resistance (Peart et al., 2002). This resulted in shorter and more branched plants (Fig. 4A), similar to the phenotype described previously (Peart et al., 2002). Taken together, these results demonstrate that *Sec5* silencing is effective and point to an important role for Sec5 in plant development.

Sec5 Silencing Enhances Susceptibility to *P. infestans* and Abolishes CRN2-Induced Cell Death Responses

To study the role of Sec5 in defense against *P. infestans*, we performed infection assays on leaves detached from *Sec5*-silenced *N. benthamiana* plants with two *P. infestans* strains, 14-3-GFP and T20-2. The results

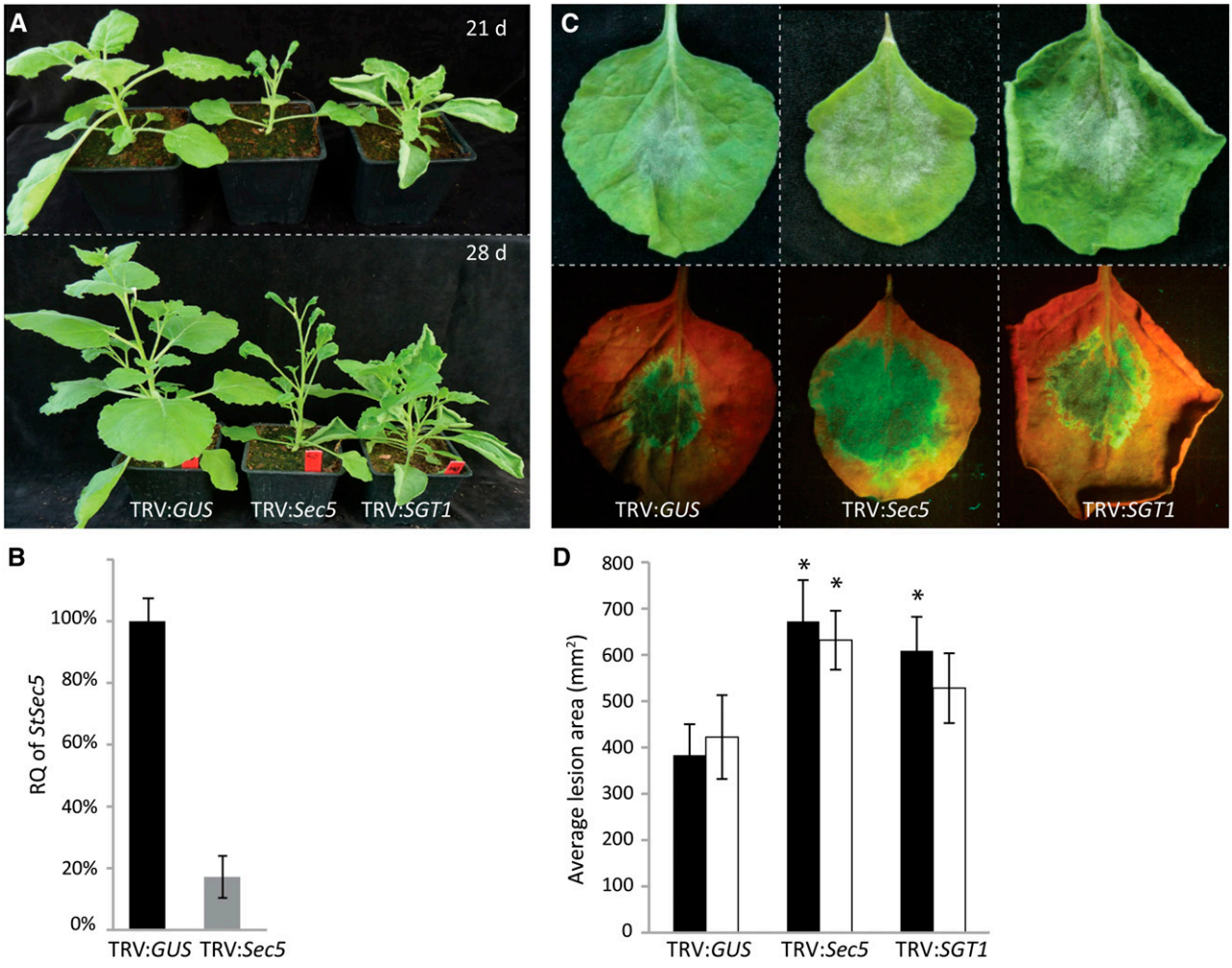

Figure 4. *Sec5*-silenced *N. benthamiana* plants show increased susceptibility to *P. infestans*. A, Morphology of *N. benthamiana* plants at 21 and 28 dai with TRV:*GUS* (control) and the silencing constructs TRV:*Sec5* and TRV:*SGT1*. B, Relative quantification (RQ) of *Sec5* expression 21 dai with TRV constructs. In the Q-RT-PCR assay, *ACTIN* expression was used for normalization. *Sec5* expression in the TRV:*GUS*-treated plants was set at 100%. The experiment was repeated three times. Error bars indicate the SE from three biological replicates. C and D, At 21 dai with TRV constructs, leaves were detached and drop inoculated with *P. infestans* zoospores. After 6 d, photographs were taken and lesion sizes were measured. C, Leaves inoculated with *P. infestans* isolate 14-3-GFP without (top) and with UV illumination (bottom). D, Lesion areas in mm^2 (*y* axis) on leaves inoculated with isolate T20-2 (black bars) and 14-3-GFP (white bars). Error bars indicate the SD from eight replicates. The experiments were repeated three times with similar results. Asterisks indicate significant differences from the control ($n \geq 8$; one-sided Student's *t* test, $P < 0.05$).

show that the lesions on *Sec5*-silenced plants are larger than the lesions on control plants (Fig. 4, C and D). Also, the *Sec5*-silenced tomato plants appeared to be more susceptible to *P. infestans* (Supplemental Fig. S8, C and D), and this indicates that, in both plant species, Sec5 is needed to counteract the pathogen.

The finding that AVR1 not only suppresses CRN2-induced cell death but also targets Sec5 raised the question of whether Sec5 has a role in CRN2-triggered cell death. To investigate this, we infiltrated leaves of *Sec5*-silenced and *SGT1*-silenced *N. benthamiana* plants with CRN2 and compared the responses at 5 dpi. As a control, we infiltrated BAX, a cell death inducer whose activity is not affected by AVR1 or A-L (Supplemental Fig. S10A). Silencing of *Sec5* clearly attenuated CNR2-triggered cell death, whereas silencing of *SGT1* had no significant effect when compared with the TRV:*GUS*-treated control plants (Fig. 5A). Moreover, neither *Sec5* silencing nor *SGT1* silencing caused a significant change in the BAX-triggered cell death response (Supplemental Fig. S10B).

To quantify the level of cell death triggered by CRN2 on *Sec5*-silenced plants, we analyzed ion leakage as a measure for plant cell death. Between 1 and 3 dpi, relative ion leakage levels in TRV:*GUS* plants had increased from approximately 25% to more than 50%, while in TRV:*Sec5* plants, there was hardly any increase (Fig. 5B). To further confirm this, we analyzed the production of reactive oxygen species (ROS), another hallmark of cell death. Hydrogen peroxide (H_2O_2) is a ROS that can be visualized with the fluorescent dye 2′,7′-dichlorodihydrofluorescein diacetate (DCFH-DA). In leaves infiltrated with an *A. tumefaciens* strain carrying a control construct (GUS) and stained with DCFH-DA, there was hardly any green fluorescence detectable, neither in control plants nor in *Sec5*- and *SGT1*-silenced plants, thus demonstrating that there was no or little H_2O_2 present (Fig. 5C). In contrast, infiltration with CRN2 resulted in strong confluent green fluorescence in control plants and *SGT1*-silenced plants, pointing to a huge increase in H_2O_2 production. In *Sec5*-silenced plants, however, the fluorescence was much weaker, with patches covering less than half of the surface; hence, production of H_2O_2 was clearly reduced. These results combined with the ion leakage data demonstrate that cell death is attenuated in *Sec5*-silenced plants and lead to the conclusion that Sec5 is required for CRN2-induced cell death.

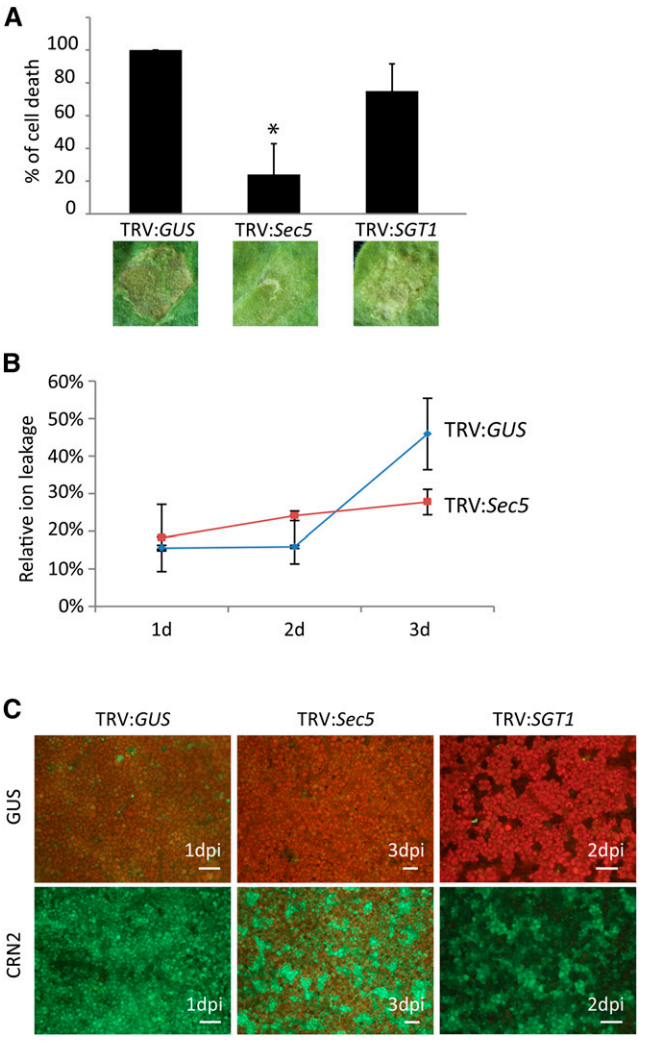

Figure 5. CRN2-triggered cell death responses are attenuated in *Sec5*-silenced *N. benthamiana* plants. A, Leaves of control (TRV:*GUS*) and *Sec5*- and *SGT1*-silenced plants were infiltrated with *A. tumefaciens* strain AGL1 harboring the construct expressing *CRN2*. Cell death development was monitored, and photographs were taken at 6 dpi. The bars reflect the average percentage of infiltrated sites that developed cell death in three independent experiments. The asterisk indicates a significant difference from the TRV:*GUS*-treated plants ($n \geq 8$; one-sided Student's *t* test, $P < 0.05$). B, Relative ion leakage (*y* axis) in leaves of control (TRV:*GUS*) and *Sec5*-silenced plants measured at 1, 2, and 3 dpi with CRN2. C, ROS production in leaves of control (TRV:*GUS*) and *Sec5*- and *SGT1*-silenced plants visualized by staining H_2O_2 with DCFH-DA and analyzed by microscopy at 1, 2, and 3 dai with GUS (as a control; top) and CRN2 (bottom). CRN2-infiltrated leaves of TRV:*GUS* (left) and *SGT1*-silenced plants (right) already showed strong fluorescence shortly after infiltration (shown are 1 and 2 dpi, respectively). In CRN2-infiltrated leaves of *Sec5*-silenced plants (middle), the fluorescence was much weaker, even at later time points (as shown at 3 dpi), pointing to a much lower H_2O_2 production compared with the controls. Bars = 200 μm.

Sec5 Is Required for the Secretion of PR-1 to the Apoplast

The exocyst, of which Sec5 is a subunit, is known to function in vesicle trafficking. In plants, the exocyst might play a role in the secretion of antimicrobial compounds, including PR proteins that are often induced upon pathogen attack. PR-1 is one of the PRs that is secreted to the apoplast and is frequently used as a marker for PTI (Wick et al., 2003; Wang et al., 2005; Kalde et al., 2007). Here, we used PR-1 as a marker to monitor the involvement of Sec5 in secretion. We exposed *Sec5*-silenced *N. benthamiana* plants (TRV:*Sec5*) and control plants to SA to induce PR-1 accumulation and subsequently analyzed PR-1 levels in the apoplast. Apoplastic fluid was collected, and proteins were

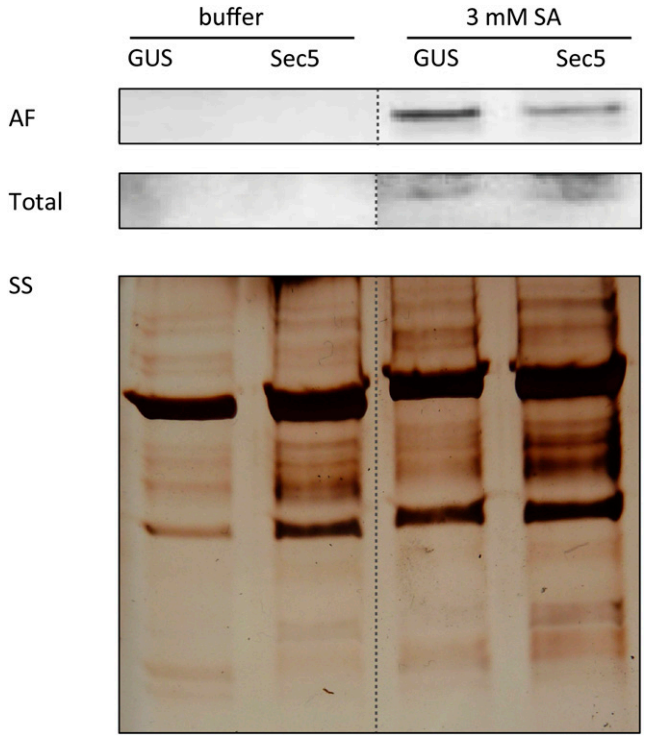

Figure 6. Sec5 is required for PR-1 accumulation in the apoplast. Immunoblots containing apoplastic fluid (AF) and total protein extract (Total) from leaves of control (GUS) and *Sec5*-silenced (Sec5) *N. benthamiana* plants treated with buffer or 3 mM SA, were probed with PR-1 antibody. The bottom part shows a section of the silver-stained (SS) gel containing proteins from the apoplastic fluid.

separated by SDS-PAGE. Western-blot analysis was performed with an antibody that is specific for PR-1 and detects a single band of 14 kD. This revealed that there was less PR-1 in apoplastic fluid collected from *Sec5*-silenced plants than in apoplastic fluid collected from control plants (Fig. 6), whereas in the total protein extracts, there was no difference. This result indicates that Sec5 contributes to PR-1 secretion to the apoplast.

AVR1 Is Able to Suppress Sec5-Dependent Callose Deposition

The increased susceptibility due to *Sec5* silencing suggests that Sec5 is required for PTI. To test this, we monitored callose deposition, another marker associated with PTI. We analyzed the level of callose deposition in *Sec5*-silenced *N. benthamiana* plants infiltrated with *Pst ΔhrcC*, the *hrcC* mutant of *Pseudomonas syringae* pv *syringae* DC3000 that can no longer secrete effectors and suppress callose deposition. Microscopic analysis revealed that control plants displayed a significant level of callose deposition at 14 h after infiltration with *Pst ΔhrcC*. In contrast, callose deposition was not observed in *Sec5*- and *SGT1*-silenced plants (Fig. 7A). Hence, it can be concluded that *Sec5* is required for callose deposition in *N. benthamiana*, indicating a role for Sec5 in PTI.

The finding that AVR1 interacts with Sec5 (Fig. 2, A and B) raised the question of the extent to which AVR1 can mimic the effect of *Sec5* silencing on PTI and callose deposition. Therefore, we analyzed callose deposition in *N. benthamiana* plants that transiently express *AVR1*. Two days after agroinfiltration with AVR1-myc, A-L-myc, or GUS-myc constructs, leaves were infiltrated with *Pst ΔhrcC* to induce callose deposition. At 14 h after infiltration, the control leaves expressing GUS-myc displayed significant levels of callose deposition, as expected. The presence of AVR1, however, impaired the callose deposition. Hardly any callose was observed, and this was strikingly different from the situation in leaves expressing *A-L* (Fig. 7B). This difference is in line with the finding that AVR1, but not A-L, can manipulate Sec5 function.

AVR1 Stabilizes Sec5 in Planta

In the western-blot analyses that were performed to demonstrate AVR1-Sec5 interaction in planta (Fig. 2B),

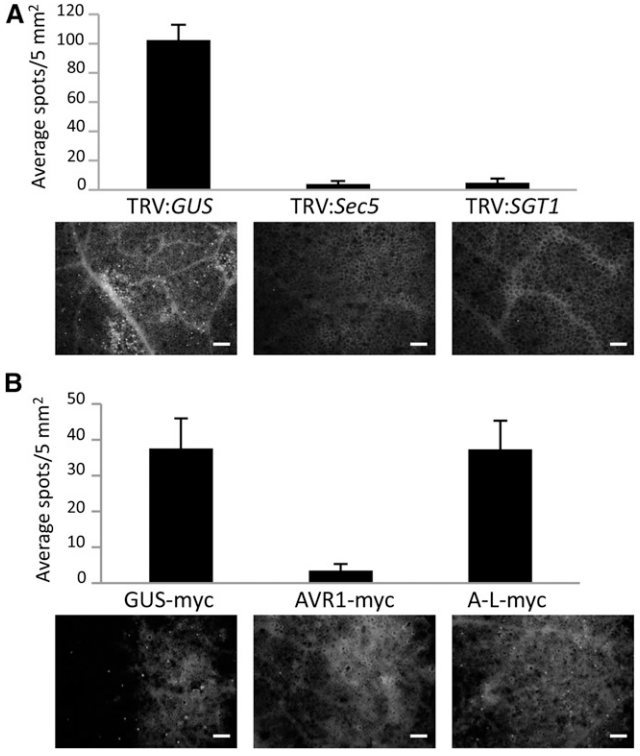

Figure 7. *Sec5* silencing and AVR1 expression impair callose deposition. Leaves from TRV:GUS-treated and *Sec5*- and *SGT1*-silenced *N. benthamiana* plants (A) and *N. benthamiana* leaves expressing GUS-myc, AVR1-myc, or A-L-myc in combination with P19 (B) were infiltrated with *Pst ΔhrcC* (1×10^8 colony-forming units mL^{-1}). After 14 h, the leaves were stained with Aniline Blue. Callose deposition was quantified by counting the number of spots per microscopy image. The bars in the graphs reflect the average number of spots per 5 mm^2 with SD based on nine replicates. Representative microscopy images are shown at the bottom. Bars = 200 μm.

GFP-StSec5 was only detected after immunoprecipitation with anti-GFP-conjugated agarose and not in the total protein extracts. This suggested that GFP-Sec5 has low steady-state levels under the experimental conditions used. To investigate whether AVR1 alters the steady-state levels of StSec5 in planta, StSec5 was coexpressed with AVR1-myc, A-L-myc, or empty vector in *N. benthamiana* leaves. Leaf samples were collected at 2, 3, and 5 dpi, and protein extracts were analyzed before and after immunoprecipitation. The results show that, after immunoprecipitation with anti-GFP-conjugated agarose, StSec5 can be detected in all samples but that the amounts vary. In the presence of AVR1, there is more StSec5 detectable than in the presence of A-L or in the empty vector control (Fig. 8). In a similar experiment, we coexpressed a GFP-HA construct with AVR1, A-L, or empty vector and observed that levels of accumulated GFP-HA were the same, irrespective of the presence of AVR1 or A-L or in the empty vector control (Supplemental Fig. S11). These results suggest that AVR1, but not A-L, affects the accumulation of StSec5 or reduces the turnover rate of the protein.

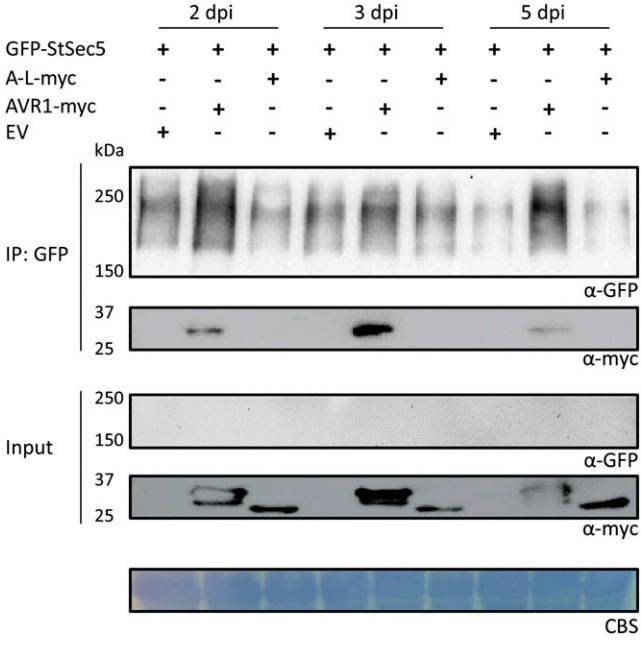

Figure 8. AVR1 stabilizes Sec5. Coexpression with AVR1 affects the steady-state levels of StSec5. Total protein extracts (Input) of *N. benthamiana* leaves 2, 3, and 5 dpi with the indicated constructs (+) and protein complexes immunoprecipitated with GFP-trap_A beads (IP: GFP) were separated on gels and blotted. GFP- and myc-tagged fusion proteins were detected by probing the blots with GFP and myc antibodies. The results shown are representative for three independent experiments. CBS, Coomassie Blue staining of the blot containing total protein extracts showed equal loading in each lane based on the 50-kD Rubisco band. EV, Empty vector.

DISCUSSION

The success of a plant pathogen is determined by its ability to overcome the intrinsic defense barriers that safeguard the plant from being attacked. In the battle between plant and pathogen, effectors play a major role. Biotrophic pathogens secrete a large variety of effectors, many of which are believed to be translocated into the host cell, where they disturb the host machinery at multiple levels. In this study, we provide evidence that one of the effectors produced by *P. infestans* targets a subunit of the exocyst complex, and this suggests that this pathogen exploits effectors to hijack exocytosis, a cellular process that is not only essential for normal plant development but also for plant defense (Hála et al., 2008; Pecenková et al., 2011). During exocytosis, secretory vesicles are directed to, and fused with, the plasma membrane, and this site-directed or focal secretion is important, for example for the formation of papillae to block pathogen penetration or for the delivery of antimicrobial compounds to infection sites to inhibit the pathogen. Indications that plant pathogens interfere with defense-related focal secretion arose from studies on fungal and bacterial pathosystems (Driouich et al., 1997; Consonni et al., 2006; Ham et al., 2006; Nomura et al., 2006) and on AVR-blb2, a *P. infestans* RXLR effector that prevents secretion of the papain-like Cys protease C14 into the apoplast (Bozkurt et al., 2011). However, none of the few RXLR host targets known so far has a direct role in the secretion machinery (Bos et al., 2010; Bouwmeester et al., 2011; Saunders et al., 2012; McLellan et al., 2013; King et al., 2014). Here, we focus on *P. infestans* AVR1, an RXLR effector that elicits a resistance response in potato plants carrying the corresponding resistance gene *R1* but subverts host defense in the absence of *R1*. To understand how AVR1 manipulates the host, we searched for host targets in a Y2H screen and identified a candidate that has a function in exocytosis. Based on our findings, we hypothesize that AVR1 indirectly abolishes callose deposition and CRN2-induced cell death by manipulating or suppressing the function of Sec5, one of the subunits of the exocyst complex. Our findings are discussed below and incorporated in a model. To our knowledge, this is the first report describing an exocyst component as a direct target of an oomycete RXLR effector.

Upon pathogen attack, the basic cell machinery is alerted and the cell starts to secrete cell wall appositions and callose to infection sites. That this type of focal secretion requires adequate functioning of the vesicle-trafficking machinery is demonstrated by the fact that mutants lacking the SNARE protein SYP121 (*pen1*) show defects in papillae formation. In *pen1*, papillae formation is delayed, resulting in compromised penetration resistance to the powdery mildew *Blumeria graminis* f. sp. *hordei* (Assaad et al., 2004; Kwon et al., 2008). Enzymes involved in the synthesis of callose, one of the structural components of papillae, are transported via vesicles toward the plasma membrane (Xu and Mendgen, 1994; Nielsen et al., 2012). Perturbation

of the exocyst complex can have an impact on papillae formation, as shown for Arabidopsis *exo70B2* mutants that display abnormal papillae with vesicular halos upon powdery mildew inoculation (Pecenková et al., 2011). These same mutants also showed increased susceptibility to *P. syringae* pv *maculicola* (Pecenková et al., 2011). A role for this particular exocyst subunit in defense is further supported by the finding that Exo70B is a target of the U-box ubiquitin ligase PUB22, which acts in concert with other ubiquitin ligases as a negative regulator of PTI (Stegmann et al., 2012). Lin et al. (2013) showed that in *N. benthamiana*, silencing of *Exo70* greatly inhibited the copper-induced ROS production in both leaves and roots. However, they did not specify which subtype of Exo70 is targeted by their VIGS construct, and this makes it impossible to interpret their data. Unlike yeast and animals, which have only one *Exo70* gene, plants have at least eight Exo70 subtypes (indicated by the suffixes A to H), with each subtype encoded by multiple paralogs. Such an expansion is often associated with a differentiation in function, and indeed, for EXO70B1 in Arabidopsis, it was shown that this subtype adopted a specific role in autophagic transport (Kulich et al., 2013). Besides defects in autophagy, e*xo70B1* mutants show small spontaneous lesions and changes in susceptibility to pathogens (Stegmann et al., 2012, 2013; Zhao et al., 2015).

Unlike Exo70, Sec5 does not have subtypes. The two *Sec5* genes present in tomato and potato and the four *Sec5* genes in the allopolyploid species *N. benthamiana* are highly homologous, and, as found for the two *Sec5* genes in Arabidopsis, it is very likely that there is functional redundancy (Hála et al., 2008). Based on this, we assume that all solanaceous Sec5 homologs analyzed in this study have the capacity to interact with AVR1. Similar to Lin et al. (2013), who studied an Exo70 subtype, we observed that depletion of an exocyst component in *N. benthamiana*, in our case Sec5, affected ROS production; ROS production triggered by CRN2 was lower in *Sec5*-silenced plants than in the controls (Fig. 5). Moreover, reducing the Sec5 levels also abolished callose deposition (Fig. 7) and increased the susceptibility to *P. infestans* (Fig. 4), demonstrating that Sec5 is directly or indirectly involved in transporting callose biosynthetic enzymes to the plasma membrane and is needed for optimal defense against *P. infestans*. The fact that callose deposition was found to be suppressed by AVR1 is consistent with the finding that AVR1 targets Sec5 (Fig. 2). Apparently, AVR1 manipulates focal secretion by interacting with Sec5. A role for Sec5 and the exocyst in focal secretion was further demonstrated by our finding that silencing of *Sec5* in *N. benthamiana* impaired the secretion of the pathogenesis-related protein PR-1 to the apoplast (Fig. 6). PRs are well known as major constituents of the antimicrobial cocktails that plants produce in response to pathogen attack. They usually have the typical N-terminal signal peptide for secretion and mainly accumulate in the apoplast (Joosten et al., 1990; Van Loon and Van Strien, 1999). Previous studies already indicated that the vesicle-trafficking machinery downstream of the exocyst is important for the focal secretion of PR-1. Depletion of the plasma membrane-specific syntaxin SYP132 in *N. benthamiana* resulted in delayed PR-1 secretion and compromised both Pto-mediated resistance and basal defense to *P. syringae* pv *tomato* (Kalde et al., 2007). In addition, expression of the pathogen-induced gene *AtSNAP33*, which encodes a transfer-SNARE that is involved in vesicle-associated secretion and associated with PEN1 and VESICLE-ASSOCIATED MEMBRANE PROTEIN721/722 (Yun et al., 2013), appeared to be correlated with PR-1 accumulation into the apoplast (Wick et al., 2003). To our knowledge, the function of PR-1 is still unknown, and there are no indications that PR-1 as such is required for defense against *P. infestans*. It should be noted that it was not our aim to unravel the role of PR-1 in the interaction; we simply used PR-1 as a marker to monitor secretion. An alternative marker is the secreted GFP marker secGFP (Batoko et al., 2000). We have used secGFP, in addition to PR-1, to monitor secretion in the presence of AVR1. We anticipated that AVR1 would indirectly, via targeting Sec5, inhibit secretion but as yet have found no evidence for that. It could well be that the transient secGFP expression is too high so that small changes are not detectable or that AVR1 is modulating a specific part of the secretory machinery for which we have no marker.

Studies in mammalian systems revealed the existence of an exocyst subcomplex that comprises Sec5 (Tan et al., 2015) and have demonstrated a role for Sec5 that seems to be independent from its role as an exocyst component. Sec5 was found to participate in Toll-like receptor-mediated innate immune signaling by interacting with and activating TANK-BINDING KINASE1 (Chien et al., 2006; Ishikawa and Barber, 2008; Simicek et al., 2013). Our data suggest a similar multifunctional role for Sec5 in plants. We observed that Sec5 is required for cell death triggered by CRN2 but not for cell death triggered by BAX (Fig. 5A), and this points to the involvement of Sec5 in some but not all of the different cellular processes that lead to cell death. Moreover, the fact that CRN2-triggered cell death was suppressed by AVR1 but not by A-L (Fig. 1) is again consistent with the specificity of the AVR1-Sec5 interaction (Fig. 2). Such specificity was also observed for the putative phosphatase BSU-like protein1 that is required for HR mediated by the NLR R2. AVR2, but not AVR2-like, was able to promote the interaction of BSU-like protein1 with R2 to initiate R2-mediated resistance (Saunders et al., 2012). Others have reported that Arabidopsis Sec5 interacts with Exo70B1, the Exo70 subtype that is involved in autophagy-related transport to the vacuole (Kulich et al., 2013), but to what extent this interaction is relevant for the function of Exo70B1 in autophagy is not known. The Sec5 comprising exocyst subcomplex in humans also functions in autophagy (Tan et al., 2015), but as far as we know, a role for Sec5 in autophagy in plants has not (yet) been reported.

P. infestans has the capacity to produce hundreds of RXLR effectors. The composition of the cocktail of

RXLR effectors varies among isolates. Some RXLR effectors are not crucial; deletions or frame-shift mutations do not affect viability or pathogenicity but help the pathogen to circumvent recognition by a host carrying a matching *R* gene (van Poppel et al., 2008; Yin et al., 2013). Their loss is likely neutralized by other effectors in the cocktail. Other RXLR effectors, however, seem to be indispensable; for example, every *P. infestans* isolate has AVR3a and AVR-blb1. In AVR3a, the variation in the pathogen population is limited to two amino acids ($AVR3a^{KI}$ or $AVR3a^{EM}$) that are the determinants for recognition by *R3a* plants (Armstrong et al., 2005). In AVR-blb1 (IPI-O), there is more variation with multiple genes in one isolate, and it is the combination of IPI-O variants that determines the compatibility or incompatibility with *Rpiblb1* plants (Champouret et al., 2009). In this respect, AVR1 resembles AVR3a and AVR-blb1; every isolate analyzed so far either has AVR1 and is recognized by *R1* plants or it has A-L and is compatible with *R1* plants. Similar to AVR1, A-L promotes virulence, but unlike AVR1, A-L does not sequester Sec5. This suggests that isolates lacking AVR1 might have other means to target vesicle trafficking for facilitating *P. infestans* colonization. It is very likely that, apart from AVR1, other RXLR effectors interfere with the vesicle-trafficking machinery to hamper host focal secretion. AVR-blb2, for example, is known to modulate the focal secretion of C14 (Bozkurt et al., 2011), and for AVR3a, Sec3, another exocyst component, was identified as a candidate host target by Y2H assay (Bos et al., 2010).

At first sight, the T-region of 38 amino acids seems to be the key determinant of AVR1. When deleted, AVR1 not only lost its virulence function, it also lost its ability to suppress CRN2-induced cell death and to interact with Sec5 (Figs. 1 and 3). More strikingly, the T-region by itself already increased virulence and suppressed CRN2-induced cell death, and when fused to A-L ($A\text{-}L^{ST}$), A-L gained the ability to suppress CRN2-induced cell death. In contrast, neither the T-region by itself nor $A\text{-}L^{ST}$ interacted with Sec5, pointing to the involvement of motifs or residues outside the T-region. Indeed, for AVR1, we showed that interaction with Sec5 not only relies on the T-region but also on the W2 motif in AVR1 (Fig. 3), and possibly certain intramolecular or intermolecular bonds need to be in place for a

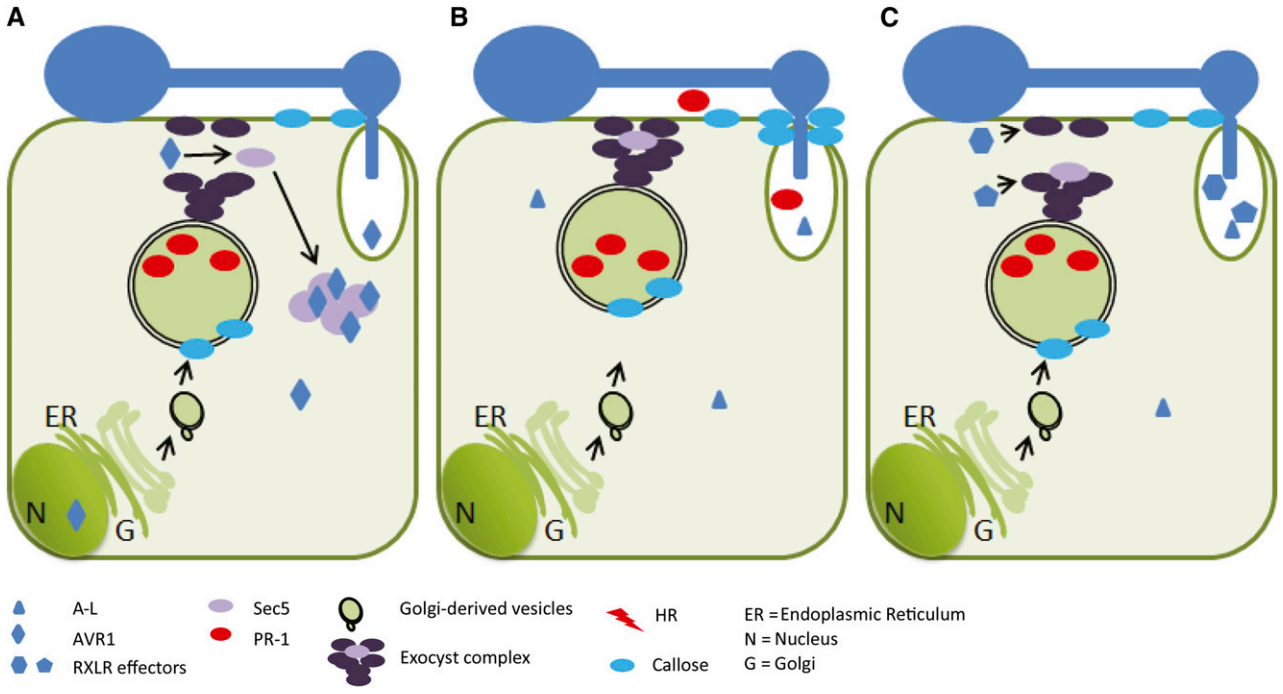

Figure 9. The *P. infestans* RXLR effector AVR1 and its host target Sec5. The models depict the interaction between AVR1 and Sec5 in plant cells colonized by *P. infestans*. Germ tubes emerging from cysts form an appressorium. After penetration, a haustorium is formed from which RXLR effectors are translocated into the host cell. A, In response to pathogen invasion, the host cell secretes antimicrobial compounds (including the pathogenesis-related protein PR-1) and deposits callose at the site of penetration to hamper infection (as depicted in B). However, when AVR1 is secreted by *P. infestans* and is translocated from the haustorium into the host cell, it targets and stabilizes Sec5 in the cytoplasm. The exocyst complex is thus out of balance and not able to mediate the focal secretion of PR-1 and callose. B, When *P. infestans* secretes A-L instead of AVR1, there is no stabilization of Sec5 by AVR1. Since colonization is not blocked, *P. infestans* can withstand the inhibitory activity of PR-1 or overcome the barrier caused by callose deposition or, as shown in C, it secretes other RXLR effectors that target the exocyst and/or vesicle-trafficking machinery to hamper the focal secretion.

proper folding to establish the interaction with Sec5. Our current studies focus at further unraveling the role of the T-region and other key determinants in AVR1 and A-L and pinpointing the subcellular localization of these RXLR effectors in relation to their host targets. In a recent study, we already showed that AVR1, when expressed in *N. benthamiana*, localizes in the nucleus and the cytoplasm (Du et al., 2015). For R1-mediated HR, which is activated when AVR1 is coexpressed with R1, nuclear localization of both components is a prerequisite. However, for suppressing CRN2-induced cell death, AVR1 needs to be in the cytoplasm, the site where Sec5 also is localized (Du et al., 2015). How this subcellular distribution is regulated is unknown.

The exocyst is a dynamic complex that guides vesicles in the cell from one site to the other. We envision that, upon infection, the plant cell activates its defense machinery by secreting antimicrobial proteins (including PR-1) into the apoplast and depositing callose at the pathogen infection site. To break this defense, *P. infestans* delivers its numerous effectors in the host cell, each of which interacts with its specific host target at different locations in the cell. AVR1 targets Sec5, binds to it, and via this interaction stabilizes the exocyst, thereby blocking the focal secretion of PR proteins and callose to the infection site (Fig. 9A). It cannot be excluded that AVR1 is unable to accomplish this stabilization on its own, because other forces may influence the behavior of Sec5 or the associated exocyst complex. There are other effectors, however, that have their own specific targets, such as other Secs (i.e. exocyst subunits), cytoskeleton proteins, or SNAREs, and in a cooperative manner they suppress defense. Unlike AVR1, A-L cannot sequester Sec5. A-L does not prevent the deposition of callose or the suppression of CRN2-induced cell death, so focal secretion may still function (Fig. 9B). Since we do not yet know the host target of A-L, we can only speculate; either A-L breaks the defense at another level, thereby overruling callose deposition, or other effectors target the exocyst and block focal secretion (Fig. 9C).

MATERIALS AND METHODS

Plant Material and Pathogen Inoculation

Nicotiana benthamiana and tomato (*Solanum lycopersicum* 'Moneymaker') were grown in a greenhouse under standardized conditions. *Phytophthora infestans* isolates 14-3-GFP, T20-2, and 88069 were maintained on rye Suc agar medium at 18°C. *P. infestans* zoospores were isolated, and detached leaf assays were performed as described previously (Champouret et al., 2009). In short, *N. benthamiana* was inoculated on the abaxial leaf surface with a 10-μL droplet of a suspension with 5×10^5 zoospores mL^{-1} and incubated at high humidity at 18°C, with the first 24 h in the dark. Lesion areas were determined at 6 dai. *Pst ΔhrcC* was grown at 28°C in King's B medium and resuspended to optical density at 600 nm of 0.5 (approximately 1×10^8 colony-forming units mL^{-1}) in 10 mM $MgCl_2$ before infiltration into *N. benthamiana* leaves (Kim et al., 2011).

Plasmid Construction

All primers used for PCR and cloning are listed in Supplemental Table S1. A 578-bp fragment of *Sec5* was PCR amplified from *N. benthamiana* cDNA using primers Sec5-vigs-F and Sec5-vigs-R and cloned into the binary vector pTRV2 using the restriction sites *Bam*HI and *Sac*I to generate TRV:*Sec5* (Supplemental Fig. S7). Potato (*Solanum tuberosum*) *StSec5* was amplified using primers Sec5F and Sec5Rwostop (Supplemental Fig. S2) from potato cDNA. Subsequently, fragments were cloned into pENTR/D-TOPO entry vector (Invitrogen) and recombined into vector pSOL2094, resulting in pSOL-StSec5 (GFP-StSec5).

P. infestans effector genes *AVR1* (PITG_16663.2), *A-L* (PITG_06432.1), *ipiO1* (PITG_21388.2; GenBank accession no. L23939.1), and *ipiO4* (GenBank accession no. GQ371191.1) were amplified without signal peptides using Gateway-compatible primers and cloned into pENTR/D-TOPO entry vector (Invitrogen). LR reactions involving various destination vectors resulted in pGWB20-*AVR1*-10myc (AVR1-myc), pGWB20-*A-L*-10myc (A-L-myc), and pGWB20-10myc (empty vector). To generate Y2H prey plasmids, pENTR vectors carrying the effector genes were recombined into pDEST32, which contains the GAL4 DNA-binding domain, resulting in pDEST32-*AVR1*, pDEST32-*A-L*, pDEST32-*ipiO1*, and pDEST32-*ipiO4*. Overlap PCR was used to generate the various deletion and chimeric constructs using appropriate primers.

AVR1:YC and A-L:YC were generated by recombining pENTR/D-TOPO entry clones containing AVR1 or A-L with pGREENII-YFPC (Zhong et al., 2008), and YN:StSec5 was generated by recombining StSec5 containing the pENTR/D-TOPO entry clone with PCL112 (Bos et al., 2010) using Gateway LR recombination.

Coding sequences of *CRN2* and *AVR1* were amplified by PCR and cloned into the binary vector pGRAB using *Not*I and *Asc*I restriction sites for *AVR1* and *Eco*RI and *Not*I for *CRN2*. Plasmids for transient expression assays were transformed into *Agrobacterium tumefaciens* strain AGL1 by electroporation.

VIGS

VIGS was performed as described previously (Peart et al., 2002). Constructs TRV:*GUS* and TRV:*SGT1* were used as controls (Tameling and Baulcombe, 2007). Two-week-old *N. benthamiana* and tomato plants were infiltrated with *A. tumefaciens* suspensions containing pTRV2 derivatives and pTRV1 in a 1:1 ratio (final optical densities at 600 nm of 1 for *N. benthamiana* and 1.6 for tomato). Three to 4 weeks later, the fifth and sixth leaves above the infiltrated leaf of *N. benthamiana*, and the fourth and fifth leaves of tomato plants, were used for further analysis.

Agroinfiltration Assays

A. tumefaciens AGL1 strains carrying binary vectors were cultured as described (Van der Hoorn et al., 2000; Champouret et al., 2009). For coexpression, we used a 1:1 ratio for all combinations. The final optical density for cell death inducers was adjusted according to the strength of the HR on *N. benthamiana*. Agroinfiltrated plants were kept in a 25°C climate chamber with a 10-h photoperiod and 70% relative humidity.

For coimmunoprecipitation experiments, leaves of *N. benthamiana* were coagroinfiltrated with GFP-StSec5 combined with AVR1-myc, A-L-myc, or empty vector and P19 (in a 1:1:1 ratio) with a final optical density of 0.3. For BiFC, *A. tumefaciens* strains harboring complementary halves of YFP were agroinfiltrated into *N. benthamiana* leaves together with P19 in a 1:1:1 ratio with a final optical density of about 0.3.

SA Treatments of *N. benthamiana* Plants and Apoplastic Fluid Isolation

N. benthamiana plants were sprayed with 3 mM SA in 20 mM sodium phosphate buffer (pH 6.5) containing 0.02% (v/v) Silwet L-77 for 4 d (El Oirdi et al., 2011). Control treatments were performed with buffer containing 0.02% (v/v) Silwet L-77 without SA. Apoplastic fluid was collected at day 4 as described by Joosten (2012).

Q-RT-PCR

Total RNA was isolated by the NucleoSpin RNA plant mini-kit (Clontech). RNA concentration was quantified, and 1 μg was used as a template for reverse transcription into cDNA with Moloney murine leukemia virus reverse transcriptase (Invitrogen) according to the manufacturer's instructions. The cDNA was diluted 10 times, and 2 μL was used per PCR with SYBR Green master mix (Promega) and gene-specific primers (Supplemental Table S1). Q-RT-PCR was

performed in triplicate on a Bio-Rad 7300 thermocycler, and gene expression was quantified and normalized to actin expression.

Y2H Assay

Yeast screening was conducted using the ProQuest two-hybrid system (Invitrogen) with pDEST32:*AVR1* as bait against a potato Y2H library as described by Bos et al. (2010). Approximately 250 His-positive yeast colonies were randomly selected in the first screening, and plasmids were isolated for sequencing. Three *StSec5* clones that were picked up in the initial Y2H screen, *StSec5-a* (pDEST22:*Sec5*$^{3\text{-}1100\ AA}$), *StSec5-b* (pDEST22:*Sec5*$^{99\text{-}1100\ AA}$), and *StSec5-c* (pDEST22:*Sec5*$^{157\text{-}1100\ AA}$), were cotransformed with pDEST32:*AVR1*, pDEST32:*A-L*, pDEST32:*ipiO1*, or pDEST32:*ipiO4*. To check their interaction strength, yeast cotransformants were first selected on synthetic defined (SD) agar plates lacking the amino acids Trp and Leu. Subsequently, cotransformants were selected on His-deficient SD plates supplemented with 25 mM 3-amino-1,2,4-triazole and uracil-deficient SD plates. Yeast controls showing strong, intermediate, and no interaction were provided by the ProQuest two-hybrid system (Invitrogen).

Staining and Microscopy

The accumulation of ROS was visualized by DCFH-DA staining. *N. benthamiana* leaves were vacuum infiltrated with a staining solution (1% DCFH-DA in dimethyl sulfoxide, diluted 1:100 in phosphate-buffered saline, pH 7.4; Rossetti and Bonatti, 2001) and incubated for 30 to 60 min. The stained tissues were then analyzed by fluorescence microscopy using a GFP filter (Nikon 90i epifluorescence microscope). Callose deposition was analyzed at 14 h after *Pst ΔhrcC* infiltration. Leaf samples were stored with ethanol to remove chlorophyll and then stained with 0.25% (w/v) aniline blue in 150 mM K_2HPO_4 (pH 9.5) for 1 h (Bouwmeester et al., 2011). Callose was visualized using epifluorescence microscopy (DAPI filter; EX340-380, DM400, BA435-4850). Three images were taken randomly from each leaf sample, and experiments were repeated three times with three replicates each time. For BiFC, a Zeiss LSM 510-Meta confocal microscope was used. The excitation wavelengths used for YFP and GFP were 514 and 488 nm, respectively. The microscopy images were taken with identical settings.

Coimmunoprecipitation and Immunoblot Analysis

N. benthamiana leaves were harvested 3 dpi and ground in liquid nitrogen. Proteins were extracted using RIPA buffer (50 mM Tris-HCl, pH 8, 150 mM NaCl, 1% Nonidet P-40 (IGEPAL CA-630), 0.5% sodium deoxycholate, and 0.1% SDS) with 5 mM dithiothreitol and one complete proteinase inhibitor tablet (Roche) per 50 mL of extraction buffer. For coimmunoprecipitation, 5 mL of total protein extract was mixed with 20 μL of GFP-trap_A beads (Chromotek) and incubated at 4°C for 1.5 h. Protein complexes attached to the beads were washed and collected, boiled for 5 min with loading buffer (300 mM Tris-HCl, pH 6.8, 8.7% SDS, 5% β-mercaptoethanol, 30% glycerol, and 0.12 mg mL^{-1} bromophenol blue), and then separated on an SDS-PAGE gel followed by transfer to an Immune-Blot polyvinylidene difluoride membrane (Bio-Rad). For the detection of myc-fused proteins, the monoclonal antibody α-myc (Sigma-Aldrich; 9E10) was used at a 1:2,000 dilution and followed by incubation with a second antibody, anti-mouse Ig-horseradish peroxidase (Amersham). For the detection of GFP-fused proteins, the antibody α-GFP (130-091-833; MACS antibodies) was used at a 1:2,000 dilution. Protein bands were detected using SuperSignal West Femto Maximum Sensitivity substrate (Thermo Scientific).

PR-1 was detected using PR-1 antibody as described by Joosten et al. (1990). Antigen-antibody complexes were detected using 1:2,000 diluted goat anti-rabbit horseradish peroxidase (Sigma-Aldrich; A9169).

Ion Leakage Measurements

From agroinfiltrated *N. benthamiana* leaves, six leaf discs (8 mm in diameter) were punched out from each infiltrated area and incubated in 4 mL of distilled water at room temperature for 2 h with slow shaking. After incubation, samples of the solution were taken for measuring sample conductivity. The leaf discs were kept in the solution and boiled for 15 min. After boiling, the solution was sampled again for total conductivity. Relative ion leakage is represented by the percentage of the sample conductivity divided by the total conductivity (Kim et al., 2003). Experiments were repeated three times with three replicates of each sample.

Supplemental Data

The following supplemental materials are available.

Supplemental Figure S1. The T-region of AVR1 is required for suppression of CRN2-triggered cell death.

Supplemental Figure S2. StSec5 protein sequence.

Supplemental Figure S3. Y2H analysis illustrating that AVR1 specifically interacts with Sec5.

Supplemental Figure S4. Mass spectrometry analysis of StSec5 immunoprecipitated with GFP-trap_A beads.

Supplemental Figure S5. Western blots showing that the AVR1, A-L, and AVR2 proteins are stable in planta.

Supplemental Figure S6. Phylogenetic tree of predicted Sec5 proteins from plants, animals, and yeast.

Supplemental Figure S7. Alignment of silencing construct TRV:*Sec5* with tomato and *N. benthamiana Sec5* sequences.

Supplemental Figure S8. *Sec5*-silenced tomato plants show increased susceptibility to *P. infestans*.

Supplemental Figure S9. In TRV:*Sec5* silenced *N. benthamiana* plants all four *Sec5* homologs are silenced.

Supplemental Figure S10. BAX-induced cell death activity is not affected by AVR1, A-L, or Sec5.

Supplemental Figure S11. AVR1 does not stabilize GFP-hemagglutinin.

Supplemental Table S1. Primers used in this study.

ACKNOWLEDGMENTS

We thank Petra C. Boevink, Patrick Smit, and Wladimir Tameling for providing plasmids; Matthieu Joosten for the PR-1 antibody; Mara de Sain, Miles Armstrong, and Elysa Overdijk for help with some of the experiments; Twan America and Jan Cordewener for performing the mass spectrometry analysis; and Tijs Ketelaar, Harold J.G. Meijer, and Rob Weide for advice and discussion. Support from the Unifarm green house facility (Henk Smit and Bert Essenstam) and the Wageningen Light Microscopy Centre (Norbert de Ruijter) is also greatly appreciated.

Received August 20, 2015; accepted August 30, 2015; published September 2, 2015.

LITERATURE CITED

Armstrong MR, Whisson SC, Pritchard L, Bos JIB, Venter E, Avrova AO, Rehmany AP, Böhme U, Brooks K, Cherevach I, et al (2005) An ancestral oomycete locus contains late blight avirulence gene Avr3a, encoding a protein that is recognized in the host cytoplasm. Proc Natl Acad Sci USA **102:** 7766–7771

Assaad FF, Qiu JL, Youngs H, Ehrhardt D, Zimmerli L, Kalde M, Wanner G, Peck SC, Edwards H, Ramonell K, et al (2004) The PEN1 syntaxin defines a novel cellular compartment upon fungal attack and is required for the timely assembly of papillae. Mol Biol Cell **15:** 5118–5129

Ballvora A, Ercolano MR, Weiss J, Meksem K, Bormann CA, Oberhagemann P, Salamini F, Gebhardt C (2002) The R1 gene for potato resistance to late blight (*Phytophthora infestans*) belongs to the leucine zipper/NBS/LRR class of plant resistance genes. Plant J **30:** 361–371

Batoko H, Zheng HQ, Hawes C, Moore I (2000) A Rab1 GTPase is required for transport between the endoplasmic reticulum and Golgi apparatus and for normal Golgi movement in plants. Plant Cell **12:** 2201–2218

Bos JIB, Armstrong MR, Gilroy EM, Boevink PC, Hein I, Taylor RM, Zhendong T, Engelhardt S, Vetukuri RR, Harrower B, et al (2010) *Phytophthora infestans* effector AVR3a is essential for virulence and manipulates plant immunity by stabilizing host E3 ligase CMPG1. Proc Natl Acad Sci USA **107:** 9909–9914

Bos JIB, Kanneganti TD, Young C, Cakir C, Huitema E, Win J, Armstrong MR, Birch PRJ, Kamoun S (2006) The C-terminal half of *Phytophthora infestans* RXLR effector AVR3a is sufficient to trigger R3a-mediated

hypersensitivity and suppress INF1-induced cell death in *Nicotiana benthamiana*. Plant J **48:** 165–176

Bouwmeester K, de Sain M, Weide R, Gouget A, Klamer S, Canut H, Govers F (2011) The lectin receptor kinase LecRK-I.9 is a novel *Phytophthora* resistance component and a potential host target for a RXLR effector. PLoS Pathog **7:** e1001327

Bozkurt TO, Schornack S, Win J, Shindo T, Ilyas M, Oliva R, Cano LM, Jones AME, Huitema E, van der Hoorn RAL, et al (2011) *Phytophthora infestans* effector AVRblb2 prevents secretion of a plant immune protease at the haustorial interface. Proc Natl Acad Sci USA **108:** 20832–20837

Champouret N, Bouwmeester K, Rietman H, van der Lee T, Maliepaard C, Heupink A, van de Vondervoort PJ, Jacobsen E, Visser RG, van der Vossen EA, et al (2009) *Phytophthora infestans* isolates lacking class I ipiO variants are virulent on Rpi-blb1 potato. Mol Plant Microbe Interact **22:** 1535–1545

Cheng BP, Yu XL, Ma ZC, Dong SM, Dou DL, Wang YC, Zheng XB (2012) *Phytophthora sojae* effector Avh331 suppresses the plant defence response by disturbing the MAPK signalling pathway. Physiol Mol Plant Pathol **77:** 1–9

Chien Y, Kim S, Bumeister R, Loo YM, Kwon SW, Johnson CL, Balakireva MG, Romeo Y, Kopelovich L, Gale M Jr, et al (2006) RalB GTPase-mediated activation of the IkappaB family kinase TBK1 couples innate immune signaling to tumor cell survival. Cell **127:** 157–170

Cole RA, Synek L, Zarsky V, Fowler JE (2005) SEC8, a subunit of the putative Arabidopsis exocyst complex, facilitates pollen germination and competitive pollen tube growth. Plant Physiol **138:** 2005–2018

Collins NC, Thordal-Christensen H, Lipka V, Bau S, Kombrink E, Qiu JL, Hückelhoven R, Stein M, Freialdenhoven A, Somerville SC, et al (2003) SNARE-protein-mediated disease resistance at the plant cell wall. Nature **425:** 973–977

Consonni C, Humphry ME, Hartmann HA, Livaja M, Durner J, Westphal L, Vogel J, Lipka V, Kemmerling B, Schulze-Lefert P, et al (2006) Conserved requirement for a plant host cell protein in powdery mildew pathogenesis. Nat Genet **38:** 716–720

Dong S, Yin W, Kong G, Yang X, Qutob D, Chen Q, Kale SD, Sui Y, Zhang Z, Dou D, et al (2011) *Phytophthora sojae* avirulence effector Avr3b is a secreted NADH and ADP-ribose pyrophosphorylase that modulates plant immunity. PLoS Pathog **7:** e1002353

Driouich A, Jauneau A, Staehelin LA (1997) 7-Dehydrobrefeldin A, a naturally occurring brefeldin A derivative, inhibits secretion and causes a *cis*-to-*trans* breakdown of Golgi stacks in plant cells. Plant Physiol **113:** 487–492

Du Y, Berg J, Govers F, Bouwmeester K (2015) Immune activation mediated by the late blight resistance protein R1 requires nuclear localization of R1 and the effector AVR1. New Phytol **207:** 735–747

El Oirdi M, El Rahman TA, Rigano L, El Hadrami A, Rodriguez MC, Daayf F, Vojnov A, Bouarab K (2011) *Botrytis cinerea* manipulates the antagonistic effects between immune pathways to promote disease development in tomato. Plant Cell **23:** 2405–2421

Evangelisti E, Govetto B, Minet-Kebdani N, Kuhn ML, Attard A, Ponchet M, Panabières F, Gourgues M (2013) The *Phytophthora parasitica* RXLR effector penetration-specific effector 1 favours *Arabidopsis thaliana* infection by interfering with auxin physiology. New Phytol **199:** 476–489

Flor HH (1971) The current status of the gene-for-gene concept. Annu Rev Phytopathol **9:** 275–296

Guo J (2008) *Phytophthora infestans* avirulence genes: mapping, cloning and diversity in field isolates. PhD thesis. Wageningen University, Wageningen, The Netherlands

Haas BJ, Kamoun S, Zody MC, Jiang RHY, Handsaker RE, Cano LM, Grabherr M, Kodira CD, Raffaele S, Torto-Alalibo T, et al (2009) Genome sequence and analysis of the Irish potato famine pathogen *Phytophthora infestans*. Nature **461:** 393–398

Hála M, Cole R, Synek L, Drdová E, Pecenková T, Nordheim A, Lamkemeyer T, Madlung J, Hochholdinger F, Fowler JE, et al (2008) An exocyst complex functions in plant cell growth in *Arabidopsis* and tobacco. Plant Cell **20:** 1330–1345

Halterman DA, Chen Y, Sopee J, Berduo-Sandoval J, Sánchez-Pérez A (2010) Competition between *Phytophthora infestans* effectors leads to increased aggressiveness on plants containing broad-spectrum late blight resistance. PLoS One **5:** e10536

Ham JH, Majerczak DR, Arroyo-Rodriguez AS, Mackey DM, Coplin DL (2006) WtsE, an AvrE-family effector protein from *Pantoea stewartii* subsp. *stewartii*, causes disease-associated cell death in corn and requires a chaperone protein for stability. Mol Plant Microbe Interact **19:** 1092–1102

Hardham AR, Cahill DM (2010) The role of oomycete effectors in plant-pathogen interactions. Funct Plant Biol **37:** 919–925

He B, Guo W (2009) The exocyst complex in polarized exocytosis. Curr Opin Cell Biol **21:** 537–542

Hsu SC, TerBush D, Abraham M, Guo W (2004) The exocyst complex in polarized exocytosis. Int Rev Cytol **233:** 243–265

Hsu SC, Ting AE, Hazuka CD, Davanger S, Kenny JW, Kee Y, Scheller RH (1996) The mammalian brain rsec6/8 complex. Neuron **17:** 1209–1219

Ishikawa H, Barber GN (2008) STING is an endoplasmic reticulum adaptor that facilitates innate immune signalling. Nature **455:** 674–678

Jiang RHY, Tripathy S, Govers F, Tyler BM (2008) RXLR effector reservoir in two *Phytophthora* species is dominated by a single rapidly evolving superfamily with more than 700 members. Proc Natl Acad Sci USA **105:** 4874–4879

Jones JD, Dangl JL (2006) The plant immune system. Nature **444:** 323–329

Joosten MH (2012) Isolation of apoplastic fluid from leaf tissue by the vacuum infiltration-centrifugation technique. Methods Mol Biol **835:** 603–610

Joosten MH, Bergmans CJ, Meulenhoff EJ, Cornelissen BJ, De Wit PJ (1990) Purification and serological characterization of three basic 15-kilodalton pathogenesis-related proteins from tomato. Plant Physiol **94:** 585–591

Kalde M, Nühse TS, Findlay K, Peck SC (2007) The syntaxin SYP132 contributes to plant resistance against bacteria and secretion of pathogenesis-related protein 1. Proc Natl Acad Sci USA **104:** 11850–11855

Kim HS, Thammarat P, Lommel SA, Hogan CS, Charkowski AO (2011) *Pectobacterium carotovorum* elicits plant cell death with DspE/F but the *P. carotovorum* DspE does not suppress callose or induce expression of plant genes early in plant-microbe interactions. Mol Plant Microbe Interact **24:** 773–786

Kim M, Ahn JW, Jin UH, Choi D, Paek KH, Pai HS (2003) Activation of the programmed cell death pathway by inhibition of proteasome function in plants. J Biol Chem **278:** 19406–19415

King SR, McLellan H, Boevink PC, Armstrong MR, Bukharova T, Sukarta O, Win J, Kamoun S, Birch PR, Banfield MJ (2014) *Phytophthora infestans* RXLR effector PexRD2 interacts with host MAPKKKε to suppress plant immune signaling. Plant Cell **26:** 1345–1359

Kroon LP, Brouwer H, de Cock AW, Govers F (2012) The genus *Phytophthora* anno 2012. Phytopathology **102:** 348–364

Kulich I, Pečenková T, Sekereš J, Smetana O, Fendrych M, Foissner I, Höftberger M, Zárský V (2013) Arabidopsis exocyst subcomplex containing subunit EXO70B1 is involved in autophagy-related transport to the vacuole. Traffic **14:** 1155–1165

Kwon C, Neu C, Pajonk S, Yun HS, Lipka U, Humphry M, Bau S, Straus M, Kwaaitaal M, Rampelt H, et al (2008) Co-option of a default secretory pathway for plant immune responses. Nature **451:** 835–840

Lewis JD, Wan J, Ford R, Gong Y, Fung P, Nahal H, Wang PW, Desveaux D, Guttman DS (2012) Quantitative interactor screening with next-generation sequencing (QIS-Seq) identifies *Arabidopsis thaliana* MLO2 as a target of the *Pseudomonas syringae* type III effector HopZ2. BMC Genomics **13:** 8

Lin CY, Trinh NN, Fu SF, Hsiung YC, Chia LC, Lin CW, Huang HJ (2013) Comparison of early transcriptome responses to copper and cadmium in rice roots. Plant Mol Biol **81:** 507–522

McLellan H, Boevink PC, Armstrong MR, Pritchard L, Gomez S, Morales J, Whisson SC, Beynon JL, Birch PR (2013) An RxLR effector from *Phytophthora infestans* prevents re-localisation of two plant NAC transcription factors from the endoplasmic reticulum to the nucleus. PLoS Pathog **9:** e1003670

Nielsen ME, Feechan A, Böhlenius H, Ueda T, Thordal-Christensen H (2012) Arabidopsis ARF-GTP exchange factor, GNOM, mediates transport required for innate immunity and focal accumulation of syntaxin PEN1. Proc Natl Acad Sci USA **109:** 11443–11448

Nomura K, Debroy S, Lee YH, Pumplin N, Jones J, He SY (2006) A bacterial virulence protein suppresses host innate immunity to cause plant disease. Science **313:** 220–223

Nomura K, Mecey C, Lee YN, Imboden LA, Chang JH, He SY (2011) Effector-triggered immunity blocks pathogen degradation of an immunity-associated vesicle traffic regulator in Arabidopsis. Proc Natl Acad Sci USA **108:** 10774–10779

Oh SK, Young C, Lee M, Oliva R, Bozkurt TO, Cano LM, Win J, Bos JIB, Liu HY, van Damme M, et al (2009) In planta expression screens of *Phytophthora infestans* RXLR effectors reveal diverse phenotypes, including activation of the *Solanum bulbocastanum* disease resistance protein Rpi-blb2. Plant Cell **21:** 2928–2947

Peart JR, Lu R, Sadanandom A, Malcuit I, Moffett P, Brice DC, Schauser L, Jaggard DAW, Xiao S, Coleman MJ, et al (2002) Ubiquitin ligase-associated protein SGT1 is required for host and nonhost disease resistance in plants. Proc Natl Acad Sci USA **99:** 10865–10869

Pecenková T, Hála M, Kulich I, Kocourková D, Drdová E, Fendrych M, Toupalová H, Zársky V (2011) The role for the exocyst complex subunits Exo70B2 and Exo70H1 in the plant-pathogen interaction. J Exp Bot **62:** 2107–2116

Rehmany AP, Gordon A, Rose LE, Allen RL, Armstrong MR, Whisson SC, Kamoun S, Tyler BM, Birch PRJ, Beynon JL (2005) Differential recognition of highly divergent downy mildew avirulence gene alleles by *RPP1* resistance genes from two *Arabidopsis* lines. Plant Cell **17:** 1839–1850

Robatzek S (2007) Vesicle trafficking in plant immune responses. Cell Microbiol **9:** 1–8

Rossetti S, Bonatti PM (2001) In situ histochemical monitoring of ozone- and TMV-induced reactive oxygen species in tobacco leaves. Plant Physiol Biochem **39:** 433–442

Saunders DGO, Breen S, Win J, Schornack S, Hein I, Bozkurt TO, Champouret N, Vleeshouwers VGAA, Birch PRJ, Gilroy EM, et al (2012) Host protein BSL1 associates with *Phytophthora infestans* RXLR effector AVR2 and the *Solanum demissum* immune receptor R2 to mediate disease resistance. Plant Cell **24:** 3420–3434

Simicek M, Lievens S, Laga M, Guzenko D, Aushev VN, Kalev P, Baietti MF, Strelkov SV, Gevaert K, Tavernier J, et al (2013) The deubiquitylase USP33 discriminates between RALB functions in autophagy and innate immune response. Nat Cell Biol **15:** 1220–1230

Stassen JH, Van den Ackerveken G (2011) How do oomycete effectors interfere with plant life? Curr Opin Plant Biol **14:** 407–414

Stegmann M, Anderson RG, Ichimura K, Pecenkova T, Reuter P, Žársky V, McDowell JM, Shirasu K, Trujillo M (2012) The ubiquitin ligase PUB22 targets a subunit of the exocyst complex required for PAMP-triggered responses in *Arabidopsis*. Plant Cell **24:** 4703–4716

Stegmann M, Anderson RG, Westphal L, Rosahl S, McDowell JM, Trujillo M (2013) The exocyst subunit Exo70B1 is involved in the immune response of Arabidopsis thaliana to different pathogens and cell death. Plant Signal Behav **8:** e27421

Synek L, Schlager N, Eliás M, Quentin M, Hauser MT, Zárský V (2006) AtEXO70A1, a member of a family of putative exocyst subunits specifically expanded in land plants, is important for polar growth and plant development. Plant J **48:** 54–72

Tameling WIL, Baulcombe DC (2007) Physical association of the NB-LRR resistance protein Rx with a Ran GTPase-activating protein is required for extreme resistance to *Potato virus X*. Plant Cell **19:** 1682–1694

Tan X, Thapa N, Sun Y, Anderson RA (2015) A kinase-independent role for EGF receptor in autophagy initiation. Cell **160:** 145–160

TerBush DR, Maurice T, Roth D, Novick P (1996) The exocyst is a multiprotein complex required for exocytosis in *Saccharomyces cerevisiae*. EMBO J **15:** 6483–6494

Torto TA, Li S, Styer A, Huitema E, Testa A, Gow NA, van West P, Kamoun S (2003) EST mining and functional expression assays identify extracellular effector proteins from the plant pathogen *Phytophthora*. Genome Res **13:** 1675–1685

Van der Hoorn RAL, Laurent F, Roth R, De Wit PJGM (2000) Agroinfiltration is a versatile tool that facilitates comparative analyses of Avr9/Cf-9-induced and Avr4/Cf-4-induced necrosis. Mol Plant Microbe Interact **13:** 439–446

Van Loon LC, Van Strien EA (1999) The families of pathogenesis-related proteins, their activities, and comparative analysis of PR-1 type proteins. Physiol Mol Plant Pathol **55:** 85–97

van Poppel PMJA, Guo J, van de Vondervoort PJ, Jung MWM, Birch PRJ, Whisson SC, Govers F (2008) The *Phytophthora infestans* avirulence gene Avr4 encodes an RXLR-dEER effector. Mol Plant Microbe Interact **21:** 1460–1470

Vleeshouwers VGAA, Raffaele S, Vossen JH, Champouret N, Oliva R, Segretin ME, Rietman H, Cano LM, Lokossou A, Kessel G, et al (2011) Understanding and exploiting late blight resistance in the age of effectors. Annu Rev Phytopathol **49:** 507–531

Wang D, Weaver ND, Kesarwani M, Dong X (2005) Induction of protein secretory pathway is required for systemic acquired resistance. Science **308:** 1036–1040

Wen TJ, Hochholdinger F, Sauer M, Bruce W, Schnable PS (2005) The *roothairless1* gene of maize encodes a homolog of *sec3*, which is involved in polar exocytosis. Plant Physiol **138:** 1637–1643

Wick P, Gansel X, Oulevey C, Page V, Studer I, Dürst M, Sticher L (2003) The expression of the t-SNARE AtSNAP33 is induced by pathogens and mechanical stimulation. Plant Physiol **132:** 343–351

Xu HX, Mendgen K (1994) Endocytosis of 1,3-beta-glucans by broad bean cells at the penetration site of the cowpea rust fungus (haploid stage). Planta **195:** 282–290

Yin W, Dong S, Zhai L, Lin Y, Zheng X, Wang Y (2013) The *Phytophthora sojae* Avr1d gene encodes an RxLR-dEER effector with presence and absence polymorphisms among pathogen strains. Mol Plant Microbe Interact **26:** 958–968

Yun HS, Kwaaitaal M, Kato N, Yi C, Park S, Sato MH, Schulze-Lefert P, Kwon C (2013) Requirement of vesicle-associated membrane protein 721 and 722 for sustained growth during immune responses in Arabidopsis. Mol Cells **35:** 481–488

Zhang Y, Liu CM, Emons AMC, Ketelaar T (2010) The plant exocyst. J Integr Plant Biol **52:** 138–146

Zhao T, Rui L, Li J, Nishimura MT, Vogel JP, Liu N, Liu S, Zhao Y, Dangl JL, Tang D (2015) A truncated NLR protein, TIR-NBS2, is required for activated defense responses in the exo70B1 mutant. PLoS Genet **11:** e1004945

Zheng X, McLellan H, Fraiture M, Liu X, Boevink PC, Gilroy EM, Chen Y, Kandel K, Sessa G, Birch PR, et al (2014) Functionally redundant RXLR effectors from *Phytophthora infestans* act at different steps to suppress early flg22-triggered immunity. PLoS Pathog **10:** e1004057

Zhong S, Lin Z, Fray RG, Grierson D (2008) Improved plant transformation vectors for fluorescent protein tagging. Transgenic Res **17:** 985–989